Reports File
Posted
ORA

GEORGIA INSTITUTE OF TECHNOLOGY
OFFICE OF RESEARCH ADMINISTRATION

RESEARCH PROJECT INITIATION

Date: February 13, 1974

Project Title: Two-Dimensional Optical Processing of One-Dimensional Signals

Project No: E-21-640

Principal Investigator: Dr. W. T. Rhodes

Sponsor: National Science Foundation

Agreement Period: From 2/1/74 Until 7/31/75*

Type Agreement: Grant No. GK-41222

Amount:

$27,700	NSF Funds (E-21-640)
4,815	GIT Contrib. (E-21-325)
$32,515	TOTAL

Reports Required: Interim Technical Reports (at least Semi-Annually);
Final Summary Report

Sponsor Contact Person (s):

Technical Matters

Elias Schutzman
Program Director,
Electrical & Optical Communications Program
National Science Foundation
Washington, D. C. 20550
Phone: (202) 632-5881

Administrative Matters

(Thru ORA)
Wilbur W. Bolton, Jr.
Grants Officer
NSF
Washington, D. C. 20550

*Proposed project period (12 mos.) ends 1/31/75; all committments to be met by grant expiration date unless formal extension is obtained in advance.

Assigned to: Electrical Engineering

COPIES TO:

- Principal Investigator
- School Director
- Dean of the College
- Director, Research Administration
- Director, Financial Affairs (2)
- Security-Reports-Property Office
- Patent Coordinator
- Library
- Rich Electronic Computer Center
- Photographic Laboratory
- Project File
- Other

351

RA-3 (6-71)

Posted
A&S
OHL

B351
NT

GEORGIA INSTITUTE OF TECHNOLOGY
OFFICE OF CONTRACT ADMINISTRATION
RESEARCH PROJECT TERMINATION

Date: December 19, 1975

Project Title: Two-Dimensional Optical Processing of One-Dimensional Signals

Project No: E-21-640

GRANT - GK-41222

Principal Investigator: Dr. W. T. Rhodes

Sponsor: National Science Foundation

Effective Termination Date: 7/31/75

Clearance of Accounting Charges: 7/31/75

Grant/Contract Closeout Actions Remaining:

Assigned to School of Electrical Engineering

COPIES TO:

- Principal Investigator
- School Director
- Dean of the College
- Office of Financial Affairs (2)
- Patent and Inventions Coordinator
- Research Services/Photo Lab ✓
- Library, Technical Reports Section
- Office of Computing Services
- Terminated Project File No. E-21-640
- Other ____

TWO-DIMENSIONAL OPTICAL PROCESSING OF ONE-DIMENSIONAL SIGNALS

BY

WILLIAM T. RHODES

JAMES M. FLORENCE

JULY 1975

TECHNICAL REPORT NO. GIT-EE-OIPL-75-1

THIS WORK WAS SUPPORTED BY THE
NATIONAL SCIENCE FOUNDATION
GRANT GK-41222

SCHOOL OF ELECTRICAL ENGINEERING
GEORGIA INSTITUTE OF TECHNOLOGY
ATLANTA, GEORGIA 30332

TWO-DIMENSIONAL OPTICAL PROCESSING OF ONE-DIMENSIONAL SIGNALS

BY

WILLIAM T. RHODES

JAMES M. FLORENCE

JULY 1975

TECHNICAL REPORT NO. GIT-EE-OIPL-75-1

THIS WORK WAS SUPPORTED BY THE
NATIONAL SCIENCE FOUNDATION
GRANT GK-41222

SCHOOL OF ELECTRICAL ENGINEERING
GEORGIA INSTITUTE OF TECHNOLOGY
ATLANTA, GEORGIA 30332

ABSTRACT

This research reported here centers on the investigation of a new class of coherent-optical processing operations for one-dimensional signals. In this class, the second degree of freedom provided by an optical system is utilized in performing operations largely new to signal processing. These operations have great potential in the development of specialized signal analysis devices--e.g. a constant relative bandwidth optical spectrum analyzer with log-frequency output display--and provide the basis for powerful frequency variant-frequency mapping signal waveform processing operations. Although the two-dimensional nature of coherent optical systems has been utilized before in the processing of one-dimensional signals, this utilization has been primarily to extend to signals of larger information content operations that can be performed by one-dimensional systems. By way of contrast, the operations reported here depend intrinsically on the two-dimensional nature of the optical system. Theoretical aspects of the research include an analytical modeling of the interaction of the different two-dimensional masks and holographic elements that serve as principal elements in the systems and a comparison of the optical techniques with other signal spectral analysis schemes. Several spectral analysis systems are investigated experimentally.

TABLE OF CONTENTS

ILLUSTRATIONS

I. INTRODUCTION

In that area of optics dealing with the coherent optical processing of one dimensional signals, e.g., speech, radar, or general communication signals, the two dimensional nature of the optical system has been viewed primarily as providing potential for greatly increased information throughout: if the optical processor depicted in Fig. 1 is capable of Fourier transforming a signal segment with time-bandwidth product equaling 10^3, then the system of Fig. 2, which utilizes the full two-dimensionality of the optical transforming operation, is capable of processing signals segments with time-bandwidth products equaling 10^6 [THOMAS; MARKEVITCH; RHODES and LIMBURG; YU].

The second degree of freedom provided by an optical system can also be used, however, to increase the kinds of operations that can be performed optically in the processing of one dimensional signals. We describe here a class of coherent optical processing operations in which the two dimensionality of the optical system is not used simply to extend to signals of larger information content operations that can be performed by one dimensional systems. Rather, the additional degree of freedom provided by the system is utilized in performing operations largely new to optical signal processing. These operations can be exploited in the design of a new class of optical spectrum analyzers. They also open an area of optical processing of signal waveforms characterized by arbitrary mappings of temporal frequency components.

II. FREQUENCY-VARIANT OPTICAL SPECTRUM ANALYZERS

In this section we describe three simple optical spectrum analyzers that illustrate certain features of this class of signal processing

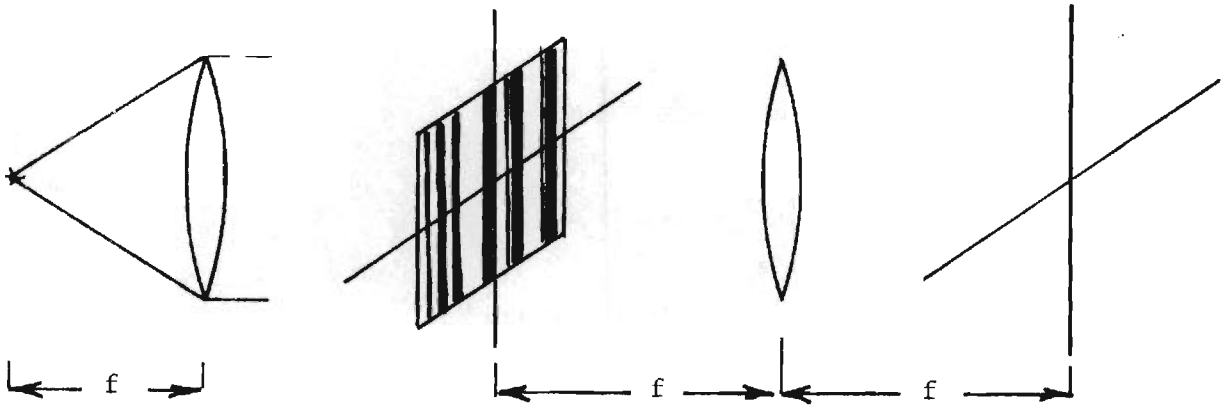

Fig. 1. Spectrum analyzer for one-dimensional signals: signal recorded in one-dimensional format. Typical optical processor can analyze 10^3 input samples (time-bandwidth product) in this format.

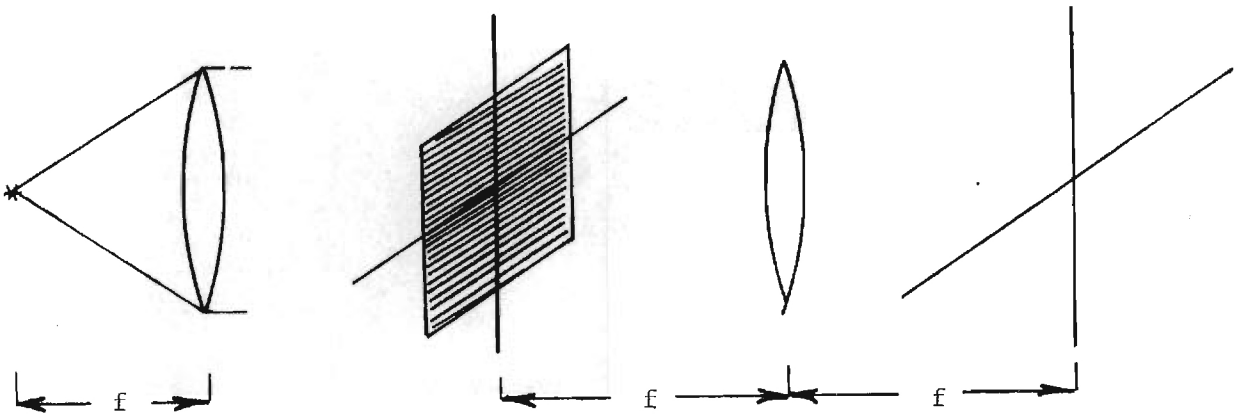

Fig. 2. Spectrum analyzer for one-dimensional signals: signal recorded in two-dimensional raster format. 10^6 samples can be processed simultaneously in this format.

operations. In discussing the systems, we shall assume that the input signal is recorded on film in the manner depicted in Fig. 3, and we shall often speak of the corresponding time or temporal-frequency characteristics of the recordings rather than of their spatial and spatial-frequency characteristics. It should be noted that these and other systems to be described are operable in real time if the input recording is replaced with one of several real-time input devices. Radio frequency signals, for example, can be input directly using a Bragg, or acousto-optic, cell. Voiceband signals can also be input in real time with a Bragg cell if a speedup-analyzer approach is employed.

The first system, illustrated in Fig. 4, is an optical spectrum analyzer characterized by frequency-dependent time and frequency resolution [W. RHODES, 1974]. This system will be recognized to be fundamentally one that images the input transparency in the vertical direction and Fourier transforms it in the horizontal direction. Such systems have been employed before for Fourier transforming in parallel a large number of recorded signals [CUTRONA]. The distinguising features in this case are the absence of multiple input signals and the use of a special input-plane mask. Here one signal serves as the input, with the length of signal present depending upon vertical position in the plane. The result is an output-plane irradiance distribution that represents the spectral content of the input signal for continuously-varying degrees of time and frequency resolution. Toward the bottom appears the spectrum of a long segment of the signal: frequency resolution is relatively good, temporal resolution relatively poor. At the top, the converse is true: temporal resolution is good and frequency resolution poor. Such a system can be quite useful in the

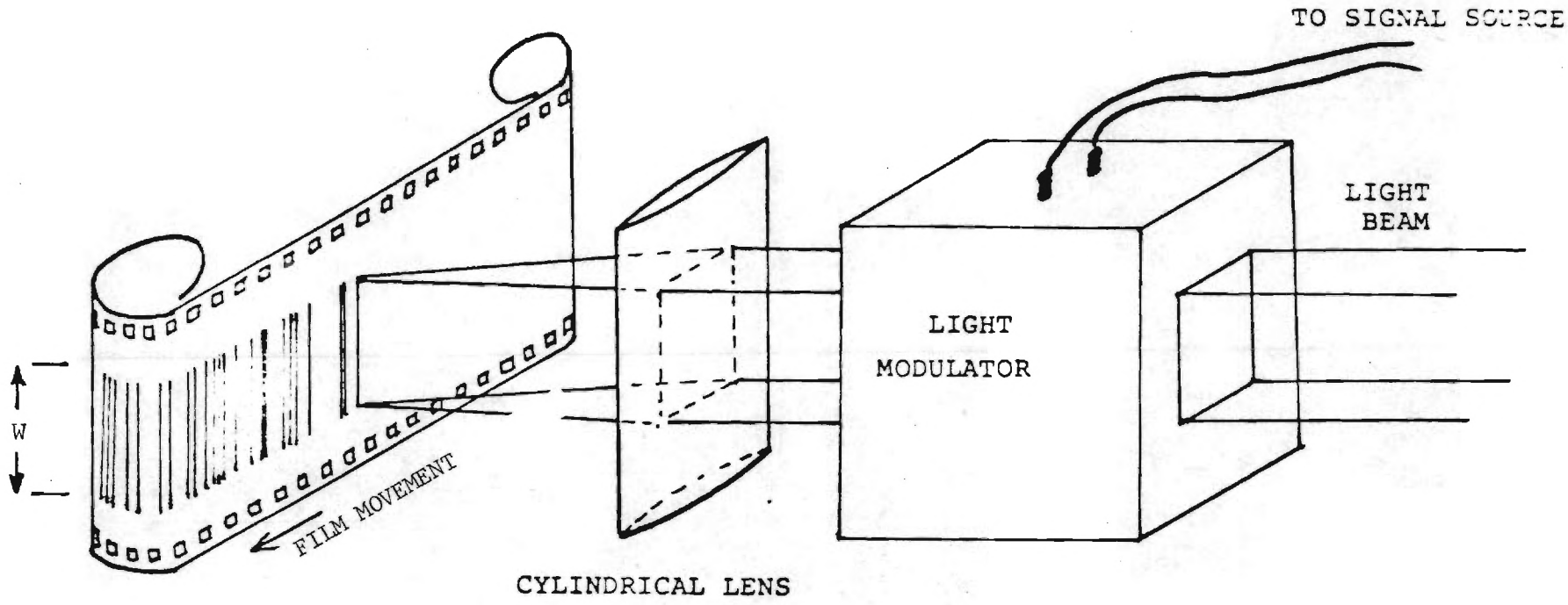

Fig. 3. Signal recording system assumed in discussion of processing operations. Modulated exposing beam is focused to narrow line having uniform intensity in vertical direction. Film is processed to yield amplitude transmittance variations proportional to applied signal.

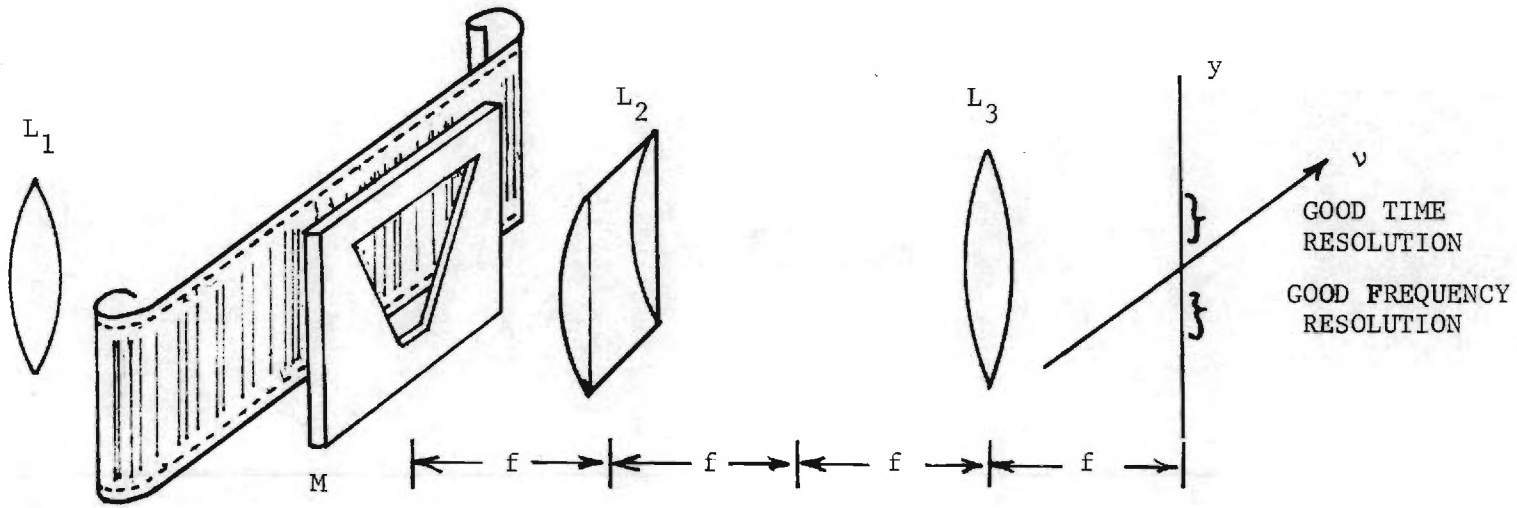

Fig. 4. Optical spectrum analyzer with continuously varying time-frequency resolution. Lens pair L_2,L_3 images input recording in vertical direction, with top-to-bottom inversion, Fourier transforms it in horizontal direction. Time resolution of spectrum for a given vertical displacement in the output plane is governed by the width, in equivalent seconds of signal record, of time-window mask M at corresponding displacement in the input plane. Frequency resolution is inversely proportional to time resolution. Mask M can assume many configurations, need not be binary.

analysis of signals such as speech waveforms. In the development of speech bandwidth or bit-rate reduction systems, for example, tradeoffs between temporal resolution, desired to locate accurately the positions of stops and plosives in the speech train; and frequency resolution, required for good-quality reproduction of voiced phonemes, are of considerable importance [FLANAGAN, p. 147; HAMMETT]. The differential-time-window spectrum analyzer can provide at once a quick and convenient look at the spectral content of input speech segments for a wide range of signal durations. Detailed characteristics of the input plane mask are a matter of choice. For example, a window function of the form $t_w(x,y) = f(xy)$ might be chosen for a display of spectral content with constant proportional bandwidth. $f(.)$ is the basic cross-sectional window function; the width of the window is proportional to $1/y$. Binary windows are easily fabricated. A tapered window, e.g., one with a gaussian transmission profile, results in reduced spectral-component side-lobes, however.

The second system, illustrated in Fig. 5, is also an optical spectrum analyzer, this one capable of displaying spectral content of the input signal vs. an arbitrary function of frequency. The lenses L_1 and L_2 are astigmatic, having twice the focusing power in the vertical direction as in the horizontal direction.* To facilitate a description of the overall operation of the system, we illustrate several intermediate steps in Fig. 6. For convenience of illustration, we assume that the desired output of the system is a display of spectral content vs. log-frequency. In the first step, the input signal transparency, Fig. 6(a), assumed to be a recording of sinusoids with

*Spherical-cylindrical lens combinations like that in Fig. 4 can also be used.

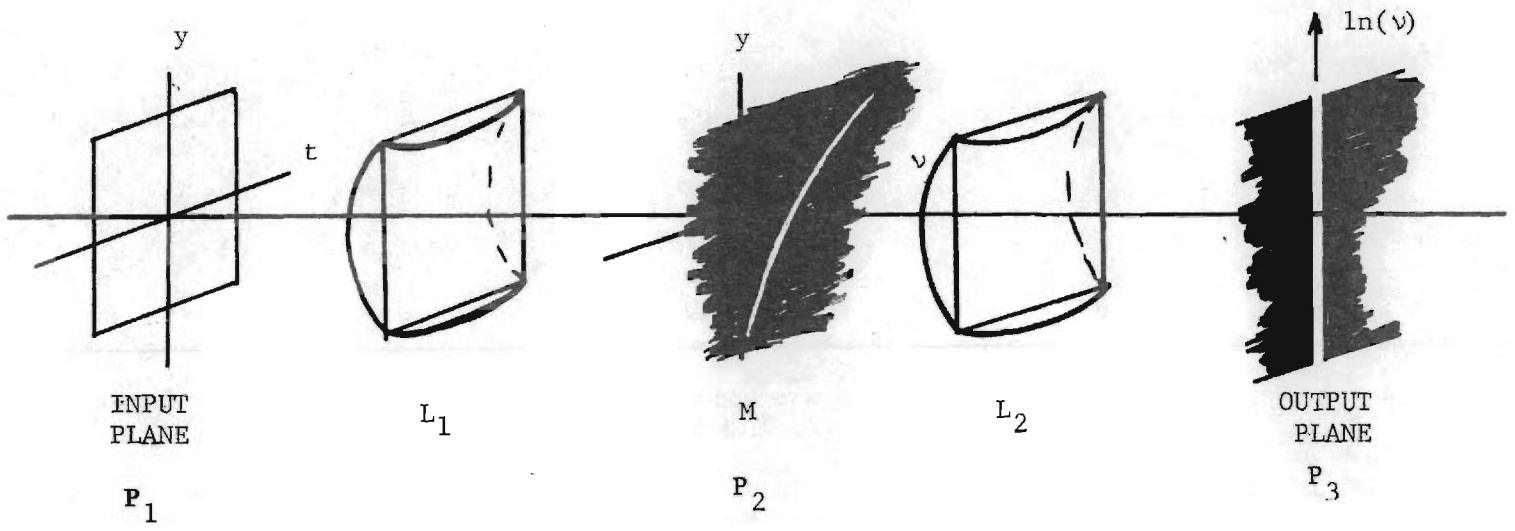

Fig. 5. Log-frequency spectrum analyzer. Lenses L_1 and L_2 are astigmatic, image in vertical direction and Fourier transform in horizontal direction. Mask M contains slit that performs log-frequency (or some other) mapping operation. Mask in output plane is opaque except along vertical axis.

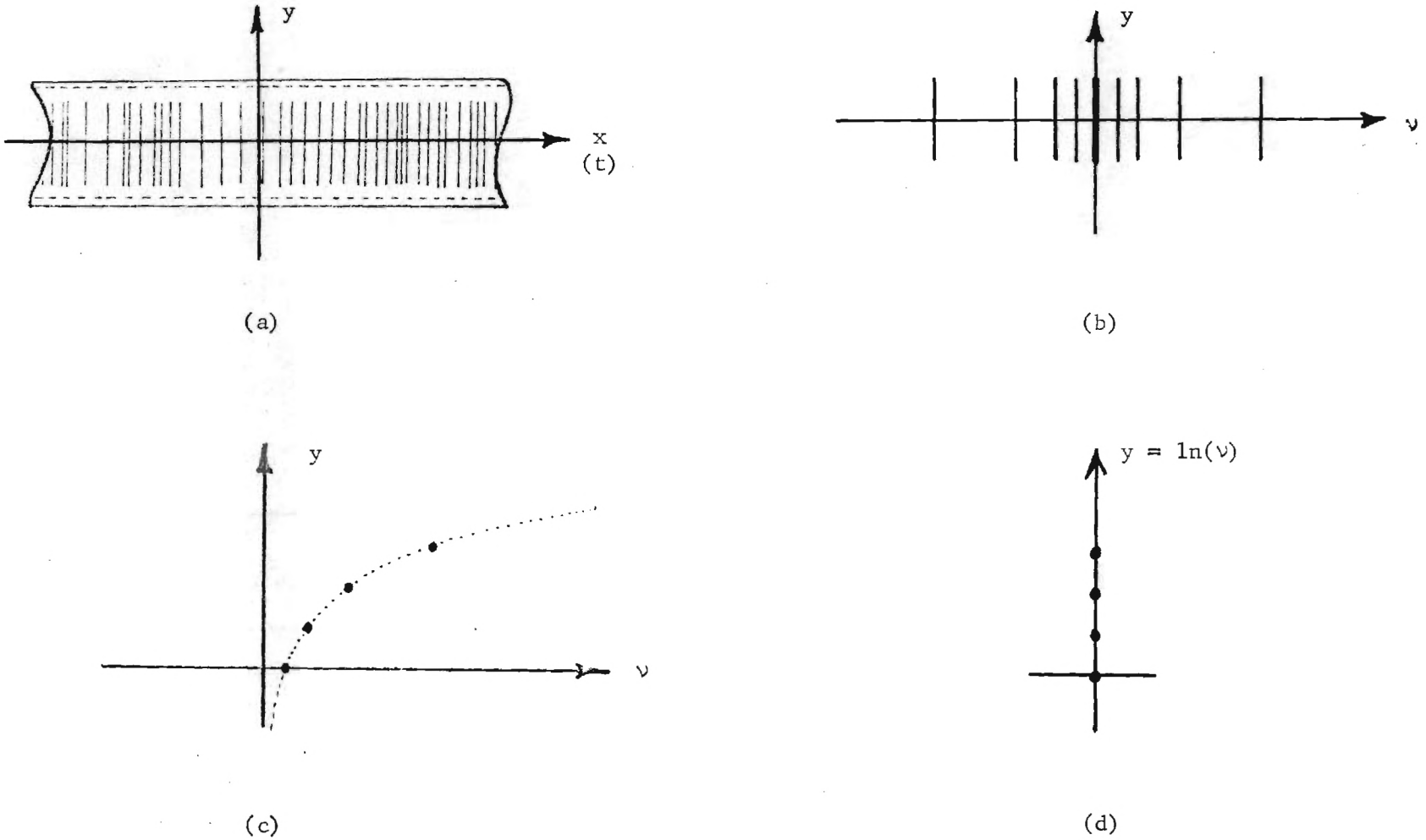

Fig. 6. Log-frequency-display optical spectrum analyzer: intermediate stages of operation. Input transparency (a) is Fourier transformed in x direction, imaged in y direction. Sinusoidal components at 1, 2, 4, and 8 cycles per unit time are displayed in (b). Mapping mask M passes only small spots of light, spaced along log curve, as shown in (c) (with different scale). Distribution along vertical axis in output plane has appearance shown in (d).

frequencies in the proportions 1:2:4:8, is Fourier transformed in the horizontal direction and imaged in the vertical direction. The resulting distribution, shown in Fig. 6(b), appears in Plane P_2 of the system. In this plane is placed a mask consisting of a narrow logarithmically curved slit. The four positive-frequency spectral components associated with the sinusoids are masked as shown in Fig. 6(c). In the final stage of the system, lens L_2 again images in the vertical direction and Fourier transforms in the horizontal direction. Each spot of light passing the mask, at its original vertical displacement from the origin (ignoring an inversion through the axis), is converted into a smear about the vertical axis. Since the light amplitude along this vertical line is proportional to the zero spatial-frequency component in the horizontal direction for each vertical displacement, masking off all but a narrow region about the vertical axis results in the amplitude distribution shown in Fig. 6(d), which displays the spectral content of the input signal vs. log-frequency. Variable attenuation in the vertical direction can be introduced by the output-plane mask to compensate for greater spot packing with large values of frequency. It is possible to display signal spectral content vs. many different functions of frequency simply by changing the functional form of the mapping slit in plane P_2. The logarithmic function is useful in many applications, but other nonlinear mappings are sometimes preferable [BRACCINI; OPPENHEIM].

A variation of this second system employs a holographic mapping element rather than the simple curved slit. Its operation, similar in some ways to the operation of coherent optical mapping systems described by BRYNGDAHL, is described in Appendix A.

The third system, which illustrates the full power of the two dimensional approach to the spectrum analysis of one dimensional signals, combines operations performed by the first two systems in a spectrum analyzer that displays spectral content vs. an arbitrary function of frequency and with frequency-dependent time and frequency resolution. The system shown in Fig. 7 is essentially that of Fig. 5, except that the input signal transparency is now masked as it is in Fig. 4. The characteristics of the mask in plane P_2 determine how spectral components are mapped; the mask in plane P_1 determines how large a time window is associated with each spectral component. Once again, detailed characteristics of the masks are a matter of choice, different applications demanding different combinations. Of particular utility is a mask combination producing a proportional-bandwidth log-frequency display of spectral content.

Figures 8 through 10 show output spectra illustrative of those obtained with the various systems discussed. Figure 8(a) shows the appearance of a single spectral line at the output of the system of Fig. 4, where the input plane window is that shown in Fig. 8(b). This window is binary with a hyperbolic (i.e., constant-Q) shape, producing an output with a $\text{sinc}^2(.)$ cross section and spectral width proportional to y. Figure 8(c) shows multiple spectral lines for the same system, where the input signal is a square wave, as shown in Fig. 8(d). No liquid gates were used in the system, accounting for spectral pattern irregularities.

In Fig. 9 is shown the output of the spectral component mapping system of Fig. 5, first with a straight-line mapping slit (Fig. 9(a)), then with a log-frequency mapping slit (Fig. 9(b)). The input was, in both cases, a square wave signal recording (ronchi-ruling).

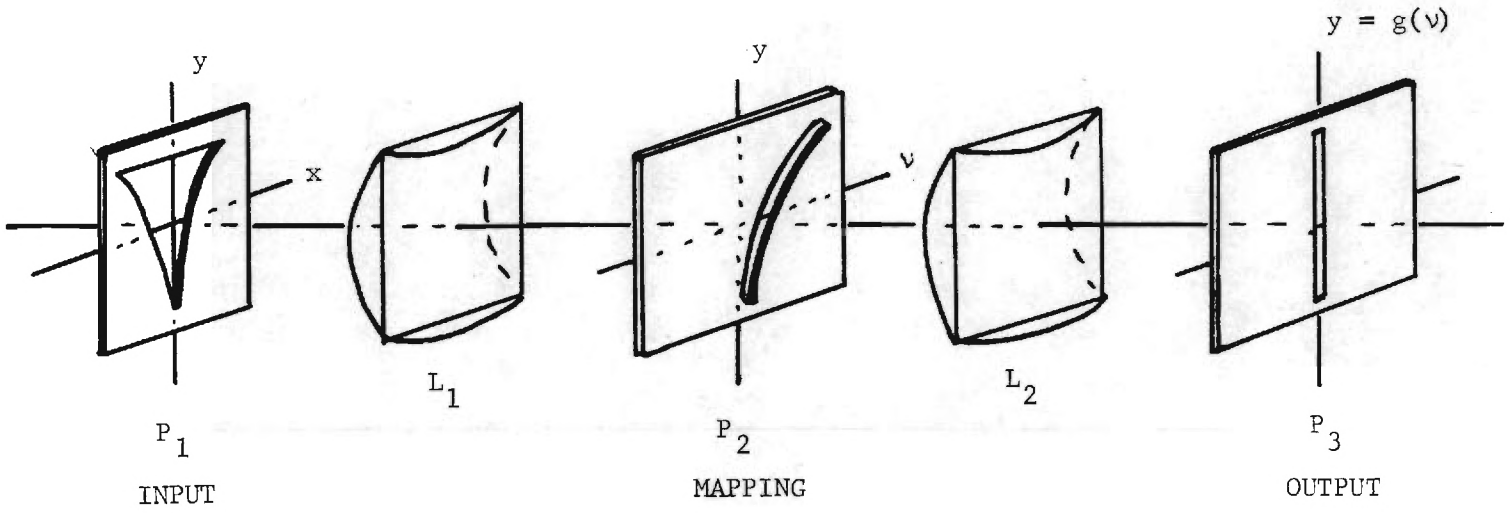

Fig. 7. Variable resolution-frequency mapping optical spectrum analyzer. Mask in plane P_1 determines time (and, consequently, frequency) resolution of system as function of frequency. Mask in plane P_2 performs general frequency mapping operation. Lenses L_1 and L_2 are again astigmatic, imaging in vertical direction, transforming in horizontal direction.

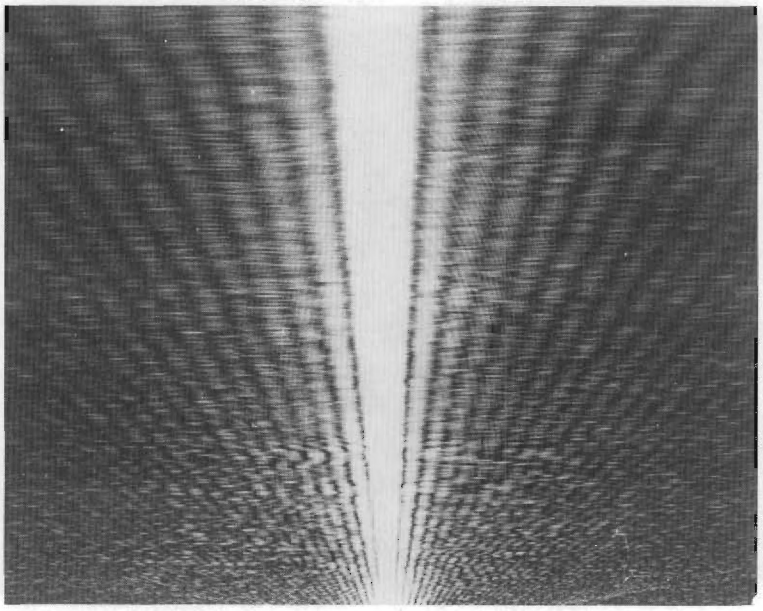

(a)

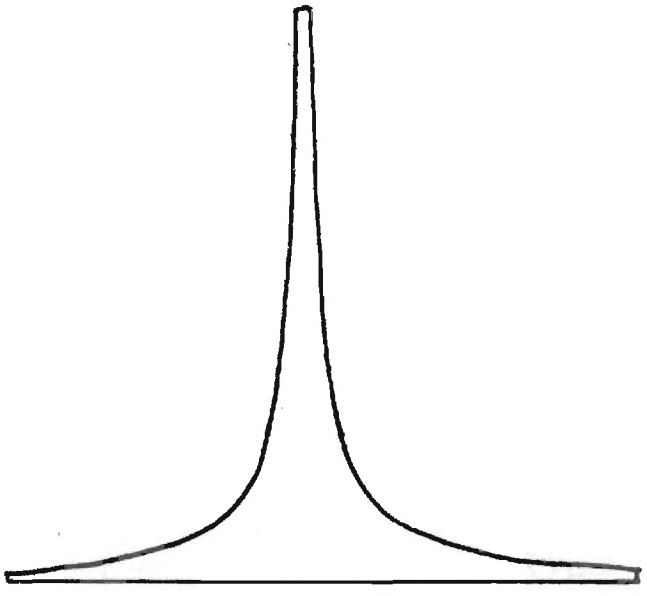

(b)

Fig. 8. Output of differential-window spectrum analyzer, (a), for single spectral component. Input window, (b), has constant proportional bandwidth characteristics.

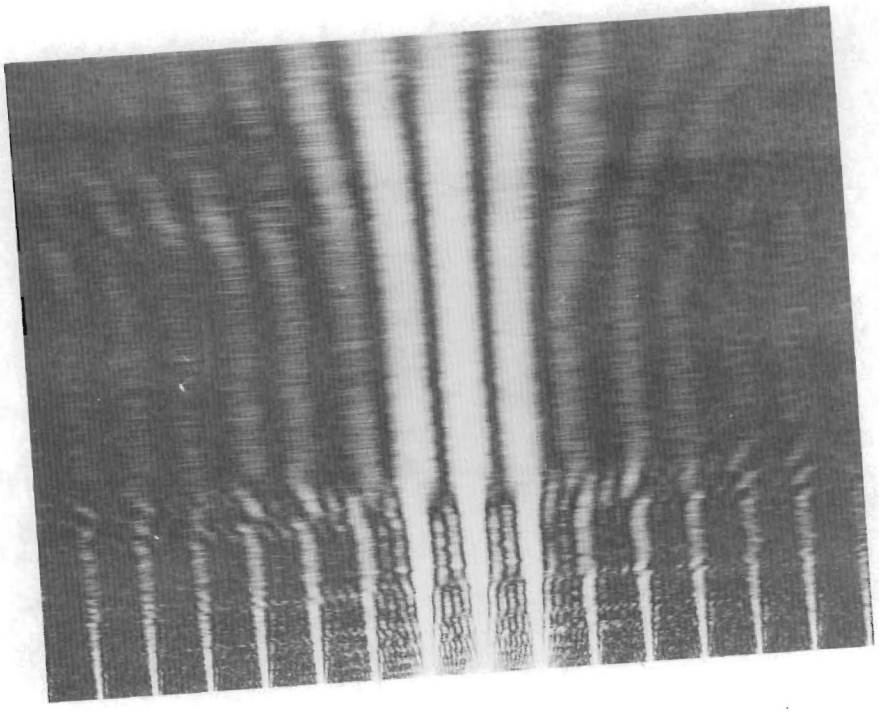

(c)

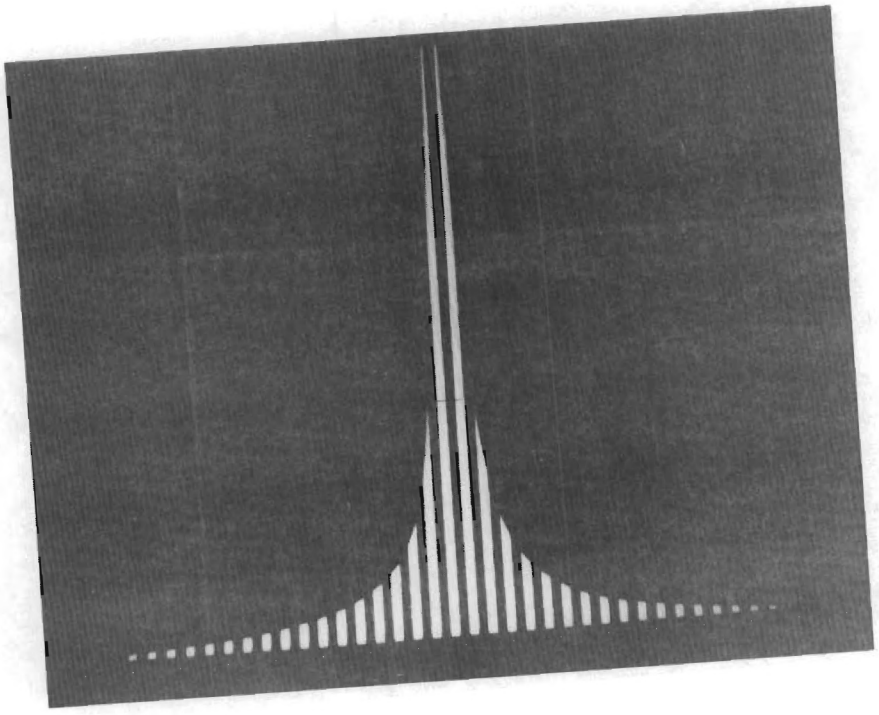

(d)

Fig. 8 cont. Output of differential-window spectrum analyzer, (c), with square wave input (ronchi ruling). Windowed input shown in (d).

Figure 10 shows the effect of combining the constant-Q input window with a log-frequency mapping slit in the system of Fig. 7. Spectral width of the high-frequency components has been broadened somewhat compared to that in Fig. 9(b).

The optical system of Fig. 7 can be used in a wide range of applications requiring a frequency-dependent, or frequency-varying, analysis of signal spectral content. If the width of the window in mask M_1 increases monotonically with y, for example, then each resolution cell in plane P_2 represents a different set of values $(\nu, \Delta\nu)$, where ν is the center frequency of the spectral component observed at that point and $\Delta\nu$ is the spectral resolution. If the mapping slit in mask M_2 is a diagonal straight line, spectral components are presented in a linear-frequency display, but with controllable resolution. The choice may be for a constant proportional bandwidth (constant-Q) analysis. Alternatively, spectral resolution can be made to change in discrete jumps, say octave by octave.

Choice of the mapping curve in mask M_2 is also flexible. There are constraints, however, imposed by the interaction of this mask with mask M_1. These constraints can be viewed as a direct consequence of the imaging nature of the overall optical system: with no mask in plane P_2, the two cylindrical-spherical lens combinations serve to image plane P_1 onto plane P_3. It is apparent that as the horizontal width of the mapping slit increases, the display at the corresponding vertical displacement in the output plane will look more like an image of the input and less like a measure of its spectral content.

Assume the mapping plane to be divided up into a large number of cells as shown in Fig. 11. In the vertical direction, cell size is determined

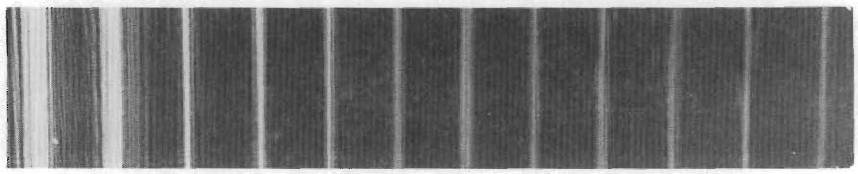

(a)

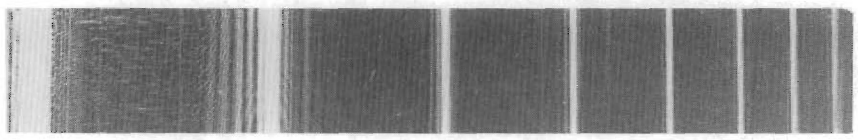

(b)

Fig. 9. Output of frequency mapping spectrum analyzer; (a) with straight line mapping slit (display linear with frequency), (b) with logarithmic mapping slit.

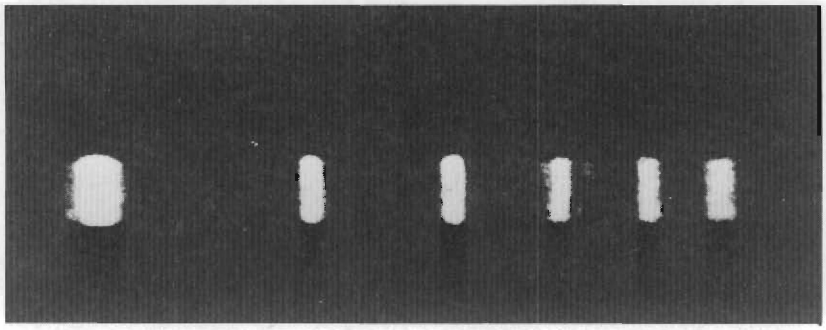

Fig. 10. Output of variable resolution-frequency mapping spectrum analyzer set up for constant-Q, log-frequency analysis.

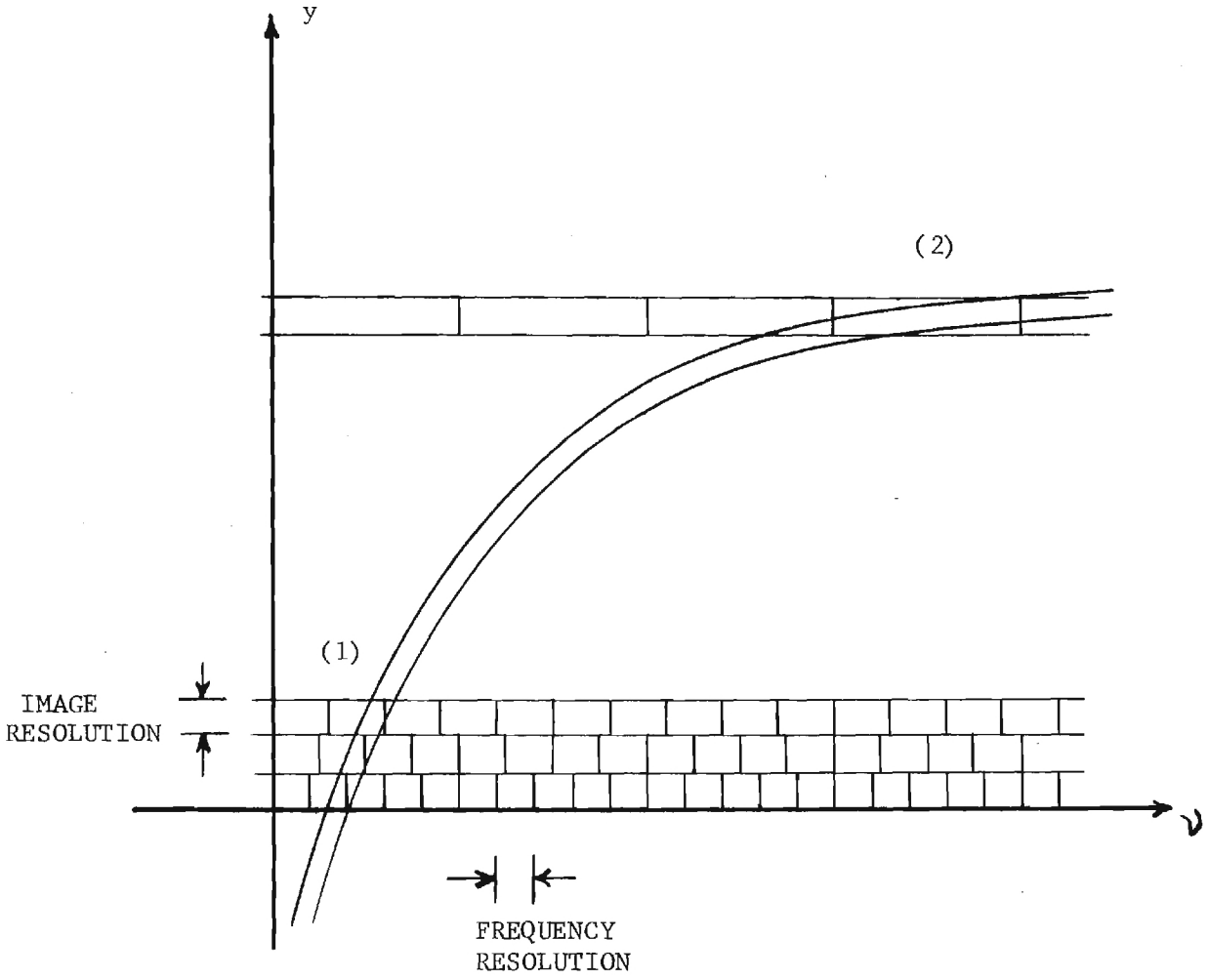

Fig. 11. Masking plane resolution cell diagram showing limitations on mapping slit width. Basic criterion is that slit pass no more than a single spectral resolution cell at each vertical location. In the example, the slit is acceptable in region (1), not in region (2).

by the resolution of the one-dimensional imaging operation, and is constant throughout the plane. In the horizontal direction, each cell has a width equal to the spectral resolution at that location, being inversely proportional to the width of the corresponding horizontal slice of the input plane mask. We take the simplifying viewpoint that, for a given vertical location, each spectral resolution cell represents an independent sample of the input signal spectral content. The basic restriction on the mapping slit in mask M_2, then, is that for each vertical location the mapping slit must have a horizontal width narrower than the spectral resolution cell it transmits. For example, the mapping slit in Fig. 11, which has a constant cross-sectional width, is satisfactory in region (1) but is unsatisfactory in region (2), where, because of its small slope, it transmits several independent spectral components. Light from these cells interferes in the output plane in a manner that depends upon the horizontal position of the input. The result is a false representation of spectral content.

It would appear that the mapping slit should be made as narrow as possible, for the chances of interference between adjacent spectral resolution cells would then be minimized. For very narrow slits, only the dimension of the image resolution cell and the slope of the slit are important in determining whether more than one spectral resolution cell (per image cell) will be transmitted. As the slit becomes narrower, however, output display brightness diminishes. A more economical approach is to choose a mapping slit whose horizontal width at any vertical location equals some constant fraction of the spectral resolution cell at that location. Such a choice still assures insignificant

interference from adjacent spectral component cells and at the same time works to equalize the output display brightness for both high resolution and low resolution spectral components.

In the following we present a brief analytical treatment of the optical systems discussed . In order to conveniently distinguish between systems, we shall refer to the spectrum analyzer of Fig. 4 as the variable resolution system, that of Fig. 5 as the frequency mapping system, and that of Fig. 7, which combines aspects of the first two, as the variable resolution-frequency mapping system.

The relationship between the complex light amplitude distribution in the input plane of the variable resolution spectrum analyzer, $u_1(x,y)$, and the output distribution, $u_2(\nu,y)$, is given by

$$u_2(\nu,y) = e^{i\alpha\nu^2} \mathfrak{F}_x\{u_1(x,y)\} , \qquad (1)$$

where the script F denotes the Fourier integral transform operation and the subscript x indicates that the operation is restricted to the variable x; ν is the corresponding frequency variable.* For simplicity in representation we have ignored various proportionality constants and scale factors (equivalent to assuming unity focal lengths and wavelength) and ignored an inversion in the y-direction associated with the one-dimensional imaging operation. The quadratic phase factor $e^{j\alpha\nu^2}$, resulting from a non-symmetric Fourier transform configuration, is

*We use ν to remind us that the observed spatial frequency distribution in the output plane is a representation of the temporal frequency content of the signal recorded on the input transparency.

easily ignored: we are ultimately interested in the output plane irradiance distribution, given by $|u_2|^2$. When necessary, the phase factor can be removed by a compensating cylindrical lens.

Assuming normally incident plane wave illumination, the input distribution, $u_1(x,y)$, is given by

$$u_1(x,y) = f(x)\, w_t(x,y) \ , \tag{2}$$

where $f(x)$ represents the recorded signal and $w_t(x,y)$ is the two-dimensional window function. Substituting into Eq. (1) we obtain the output plane distribution

$$u_2(\nu,y) = \int_{-\infty}^{\infty} F(\xi)\, W_t(\nu-\xi,y)d\xi \ , \tag{3}$$

where

$$F(\nu) = \mathcal{F}_x\{f(x)\} \tag{4}$$

and

$$W_t(\nu,y) = \mathcal{F}_x\{w_t(x,y)\} \ . \tag{5}$$

The convolution integral of Eq. (3) represents a smoothing of the signal transform $F(\nu)$, where the nature of the smoothing function depends on vertical position y.

As an example, let the input signal be a single cisoid:

$$f(x) = e^{i2\pi\nu_o x} \tag{6}$$

(representing, for example, the positive frequency component of a sinusoid recorded on film). The resulting output distribution is then

$$\begin{aligned} u_2(\nu,y) &= \int_{-\infty}^{\infty} \delta(\xi-\nu_o)\, W_t(\nu-\xi,y)d\xi \\ &= W_t(\nu-\nu_o,y) \ , \end{aligned} \tag{7}$$

which, for any particular value of y, is simply a displaced version of the transform of the corresponding cross sectional window profile. Of special interest is the case where the window is a function of the product xy; i.e.,

$$w_t(x,y) = w_t(xy) \tag{8}$$

Then the output assumes the form

$$u_2(\nu,y) = \frac{1}{y} W_t\left(\frac{\nu-\nu_o}{y}\right) \quad . \tag{9}$$

The width of the input window, and therefore the time resolution, is proportional to 1/y; the width of the resulting output display, and therefore the frequency resolution, is proportional to y. In some applications a more general resolution versus y relationship may be desirable. $w_t(x,y)$ can then be specified by $w_t(x/\Delta(y))$, where $\Delta(y)$ specifies the window width for a given y.

For this system, as for the other systems considered, the input signal recording can be moved through the input window for a delayed real-time spectral analysis operation. f(x) then becomes f(x+vt) in the analysis, where v is the recording transport velocity.

The frequency mapping spectrum analyzer of Fig. 5 can be treated as a special case of the variable resolution-frequency mapping spectrum analyzer of Fig. 7. We therefore go directly to an analysis of this latter system.

The input to the variable resolution-frequency mapping spectrum analyzer is the same as that for the system just analyzed, and $u_1(x,y)$ is given by Eq. (2). The resultant distribution incident on the mapping mask in the intermediate plane (Plane P_2 in Fig. 7) is given

by Eq. (3), which we rewrite in the form

$$u_2(\nu,y) = F(\nu) * W_t(\nu,y) \ , \tag{10}$$

where "*" is understood to denote the one-dimensional convolution operation with respect to the variable ν. The mask in the intermediate plane is assumed initially to consist of an opaque background with a very narrow transparent slit that follows the curve $y = g(\nu)$. In most cases of interest, $g(\nu)$ will be a strictly increasing monatonic function of ν with a unique inverse, $g^{-1}(\cdot)$. For convenience of notation, we define the mapping curve by the pair of equivalent equations

$$y = g(\nu) \ , \tag{11}$$

$$\nu = g^{-1}(y) = h(y) \ , \tag{12}$$

We assume the mapping slit to have a constant width in the direction of the curve normal, a typical situation. The light amplitude transmittance of the mask can then be represented by the function

$$t_m(\nu,y) = m(y)\ \delta(\nu-h(y)) \ , \tag{13}$$

where the factor $m(y)$ is given by

$$m(y) = \sqrt{1 + \left(\frac{dh}{dy}\right)^2} \tag{14}$$

(see, e.g., PAPOULIS, 1968, pg. 95). For a given y, $m(y)$ is proportional to the width of the slit in the horizontal (ν) direction.

The amplitude distribution immediately behind the mask is

$$u_2'(\nu,y) = [F(\nu) * W_t(\nu,y)]\ m(y)\ \delta(\nu-h(y)) \ . \tag{15}$$

The final stage of the optical system performs a second vertical image-horizontal transform operation, with a resulting output plane distribution

$$u_3(x,y) = \mathcal{F}_\nu^{-1}\{[F(\nu) * W_t(\nu,y)]m(y)\ \delta(\nu-h(y))\}$$

$$= [f(x)\ w_t(x,y)] * [m(y)e^{i2\pi h(y)x}] , \qquad (16)$$

where the convolution operation is with respect to the variable x. We are concerned with the portion of this distribution that lies along the line $x = 0$. Writing out the convolution integral and setting $x = 0$, we obtain

$$u_3(0,y) = \int_{-\infty}^{\infty} f(\xi)\ w_t(\xi,y)\ m(y)e^{-i2\pi h(y)\xi} d\xi . \qquad (17)$$

Equation (17) is seen to have the basic form of a Fourier transform integral. Specifically, for any position y along the vertical axis, $u_3(0,y)$ represents the spectral content of the input signal f(x) at the frequency $\nu = h(y)$, f(x) being windowed by the function $w_t(x,y)\ m(y)$. The factor m(y) reflects the greater packing of spectral components along the y-axis in regions where the slope of the mapping slit is small. (If the slit is constructed to have uniform horizontal width as a function of y, m(y) will then be constant.)

As an example, let the intermediate plane mask consist of a constant width slit along the line $y = \nu$. The inverse function, h(y), is then y, and the output is a conventional (i.e., linear with ν) display of signal spectral content with frequency-dependent time and frequency resolution. Of special interest is the case of a constant proportional bandwidth or constant Q analysis, where the frequency

resolution is proportional to frequency: $\Delta\nu \propto \nu$. From our earlier analysis, we know that an input window function of the form $w_t(xy)$ provides us with a spectral display where frequency resolution is proportional to y. Thus, by using this type of input window and the linear slit, we have a linear frequency-constant Q spectrum analyzer.

Assume now that we wish to retain the constant Q feature of the analysis but to display the spectral distribution vs. $\ln(\nu)$. How do we determine the width of the input window as a function of y? Let $w_t(x,y)$ be given by

$$w_t(x,y) = w_t\left(\frac{x}{\Delta(y)}\right) . \tag{18}$$

As a function of y, frequency resolution is proportional to $1/\Delta(y)$. For the log-frequency display we require that the slit lie along the line $y = \ln(\nu)$. We therefore have

$$y = g(\nu) = \ln(\nu) \tag{19}$$

and

$$\nu = h(y) = e^{y} . \tag{20}$$

For a constant-Q analysis, we must have frequency resolution proportional to frequency; i.e.,

$$\frac{1}{\Delta(y)} \propto e^{y} , \tag{21}$$

or

$$\Delta(y) \propto e^{-y} . \tag{22}$$

A similar approach can be taken for other resolution and mapping requirements.

As suggested earlier in this report, an infinitesimally narrow mapping slit passes an infinitesimal amount of light. We must thus consider the effect of a finite-width mapping slit on the output distribution. We return to an expression for the light amplitude distribution immediately in front of the intermediate plane mask,

$$u_2(\nu,y) = \mathcal{F}_x\{g(x)\ w_t(x,y)\} \ , \tag{23}$$

and assume a mapping transmittance function of the form

$$t_m(\nu,y) = W_f(\nu-h(y),y) \ . \tag{24}$$

This is the function $W_f(\nu,y)$ shifted by an amount ν_o, where $\nu_o = h(y)$. The amplitude distribution immediately behind the mask is then

$$u_2'(\nu,y) = \mathcal{F}_x\{f(x)\ w_t(x,y)\}\ W_f(\nu-h(y),y) \ , \tag{25}$$

and the distribution in the output plane is

$$\begin{aligned} u_3(x,y) &= \mathcal{F}_\nu^{-1}\{\mathcal{F}_x\{f(x)\ w_t(x,y)\}W_f(\nu-h(y),y)\} \\ &= [f(x)\ w_t(x,y)] * [w_f(x,y)e^{i2\pi h(y)x}] \ , \end{aligned} \tag{26}$$

where

$$w_f(x,y) = \mathcal{F}_\nu^{-1}\{W_f(\nu,y)\} \ , \tag{27}$$

and where the convolution is with respect to the variable x. Writing out the integral expression and setting $x = 0$ (again, we observe the output along the y-axis), we obtain

$$u_3(0,y) = \int_{-\infty}^{\infty} f(\xi)\ w_t(\xi,y)\ w_f(-\xi,y)e^{-i2\pi h(y)\xi}d\xi \ . \tag{28}$$

The output distribution for a given value y is seen to be the spectral content at frequency $\nu = h(y)$ with time and frequency resolution determined by an equivalent input window function, $w(x,y)$, given by

$$w(x,y) = w_t(x,y)\ w_f(-x,y)\ . \tag{29}$$

So long as the mapping slit is sufficiently narrow (the δ-function representation of Eq. (13) is then appropriate), $w_f(-x,y)$ will be quite broad in the x-direction, and resolution will be determined primarily by the input plane window. If, on the other hand, $W_f(\nu,y)$ becomes too broad in the ν direction, $w_f(x,y)$ can be approximated by a δ-function in Eq. (25) with the result

$$u_3(x,y) \propto \int_{-\infty}^{\infty} f(\xi)\ w_t(\xi,y)\ \delta(x-\xi)e^{i2\pi h(y)(x-\xi)}d\xi$$

$$\propto f(x)\ w_t(x,y)\ ; \tag{30}$$

i.e., the output plane distribution is simply an image of the masked input recording.

The description presented in this section are intended to convey a general understanding of the operation and the limitations of this class of signal analysis system. It has not been our purpose to specify design parameters; anyone skilled in the area of Fourier optics is capable of determining pertinent focal lengths and scale factors, and the choice of input window or mapping slit profiles--whether they should be binary or tapered, gaussian or raised cosine--relates to signal analysis topics adequately discussed elsewhere [JENKENS and WATTS; KARKEVITCH; PAPOULIS 1972, 1973; STARK and DIMITRIADIS]. The systems

described enjoy relative ease of construction--interferometric accuracy in the positioning of components is not necessary--and the two masks that control the frequency-varying operations can be specified with great flexibility. In all, these systems represent a potentially very useful development in the area of optical signal processing.

III. TIME-FREQUENCY SIGNAL REPRESENTATIONS

It has been suggested in the preceding section that the input signal recording may be moved in the input plane, with the output distribution then representing the time evolution of the spectral content of the recorded time waveform. Such an operation is fundamental to general areas of signal processing, perhaps the most important example being in the area of speech processing. The combined time-frequency representation of a signal f(t) given by

$$F_w(\nu,t) = \int_{-\infty}^{\infty} f(x+vt)\, w(x) e^{-i2\pi\nu x} dx \tag{31}$$

is generally referred to as the short-time amplitude spectrum of f(t). It is the starting point for many speech bit-rate reduction systems; its magnitude is the so-called spectrogram used extensively in speaker recognition [FLANAGAN]. Equation (31) represents an operation that can be performed by a one-dimensional system, and is to be contrasted with the two-dimensional operation

$$G_w(\nu,t) = \int_{-\infty}^{\infty} f(x+vt)\, w(x,\nu) e^{-i2\pi\nu x} dx \ . \tag{32}$$

In this second operation, the characteristics of the sliding window

function w( ) change as a function of frequency; time resolution and, consequently, frequency resolution become frequency variant. This second expression is characteristic of the variable-resolution spectrum analyzer discussed in Section II. The most general spectral analysis, characteristic of the variable resolution-frequency mapping spectrum analyzer, can be represented by the expression

$$S_w(\boldsymbol{\nu}(y),t) = \int_{-\infty}^{\infty} f(x+vt)\ w(x,\nu)e^{-i2\pi\nu x}dx\ , \qquad (33)$$

where the function $\nu(y)$ represents an arbitrary warping of the frequency (y) axis scale. Such operations have been referred to collectively as unequal bandwidth-frequency warping spectral analysis operations [BRACCINI and OPPENHEIM]. They can be performed digitally, but only with considerable computational difficulty, except in special cases. Optical implementation is, on the other hand, as noted, relatively simple.

Equations (31)-(33) represent three of a large number of methods developed for representing a signal in a combined time-frequency domain. As Dennis Gabor pointed out in his classic 1948 paper on the "Theory of Communication," signals like speech and music, which we perceive as having a definite time-frequency pattern, are not satisfactorily represented by either a time waveform, f(t), or its Fourier transform, $F(\nu)$, to the extent that these representations satisfy our physical intuitions [GABOR]. Gabor was the first of a number of investigators to devise a representation that made explicit the time evolution of the frequency content of a signal. Gabor's approach was to expand the signal into the sum of what he termed elementary signals.

Each elementary signal, a sinusoidal pulse with Gaussian envelope, is characterized by a center frequency and mean epoch, occupying a minimum area (determined by the time-frequency uncertainty product, $\Delta t \Delta \nu$) in the time-frequency plane. Gabor's work was made exact by HELSTROM and expanded upon by MONTGOMERY and REED and by LERNER. A different approach to the representation problem was developed by RIHACZEK, who described a signal in terms of a complex time-frequency energy density function.

We have studied these different signal representations to determine their applicability to a description of the optical spectral analysis operations discussed and to signal processing operations to be described in the next section. All but Rihaczek's representation, though conceptually useful, involve lengthy calculations that lead to results not consistent with simple interpretation. The time-frequency energy density representation, on the other hand, proves to be not only more amenable to manipulation but also to give results consistent with the operations performed by the optical systems investigated.

The complex time-frequency energy density function $\underline{\in}(t,\nu)$ associated with a particular signal $f(t)$ is defined by

$$\underline{\in}(t,\nu) = \underline{f}(t)\, \underline{F}^*(\nu) e^{-i2\pi\nu t} , \tag{34}$$

where $\underline{f}(t)$ is the complex* (analytic signal) representation of the signal [see, e.g., ACKROYD, 1970], and $\underline{F}^*(\nu)$ is the complex conjugate of the Fourier transform of $\underline{f}(t)$. It follows from the definition of

---

*We use an underbar throughout this section to denote the complex signal representation. A corresponding real time-frequency energy density can be defined by $e(t,\nu) = f(t)\, \mathrm{Re}\{F(\nu)e^{j2\pi\nu t}\}$, where $f(t)$ is the real signal waveform and $F(\nu)$ its Fourier transform [ACKROYD, 1970].

$\underline{\in}(t,\nu)$ that integration over all t gives the energy density spectrum of the signal:

$$\int_{-\infty}^{\infty} \underline{\in}(t,\nu)dt = \underline{F}^*(\nu) \int_{-\infty}^{\infty} \underline{f}(t)e^{-i2\pi\nu t}dt = |\underline{F}(\nu)|^2 \ . \qquad (35)$$

Similarly, integration over all ν gives the energy density (power) waveform of the signal:

$$\int_{-\infty}^{\infty} \underline{\in}(t,\nu)d\nu = \underline{f}(t) \int_{-\infty}^{\infty} \underline{F}^*(\nu)e^{-i2\pi\nu t}dt = |\underline{f}(t)|^2 \ . \qquad (36)$$

Also, since either the energy density spectrum or the energy density waveform can be used to determine the total signal energy, E, from

$$E = \frac{1}{2}\int_{-\infty}^{\infty} |\underline{F}(\nu)|^2 d\nu = \frac{1}{2}\int_{-\infty}^{\infty} |\underline{f}(t)|^2 dt \ , \qquad (37)$$

it follows from Eqs. (35)-(37) that integration of $\underline{\in}(t,\nu)$ over the entire time-frequency plane gives the total signal energy:

$$E = \frac{1}{2}\int_{-\infty}^{\infty}\int \underline{\in}(t,\nu)dtd\nu \ . \qquad (38)$$

The time-frequency energy density can also be used to determine the signal energy content in any time as frequency interval. From Eq. (35) the energy in this frequency interval $\Delta\nu$ centered at ν_o is given by

$$E_{\Delta\nu} = \frac{1}{2}\int_{\nu_o - \frac{\Delta\nu}{2}}^{\nu_o + \frac{\Delta\nu}{2}} |\underline{F}(\nu)|^2 d\nu = \frac{1}{2}\int_{\nu_o - \frac{\Delta\nu}{2}}^{\nu_o + \frac{\Delta\nu}{2}}\int_{-\infty}^{\infty} \underline{\in}(t,\nu)dtd\nu \ . \qquad (39)$$

Similarly, from Eq. (36), the energy in the time interval Δt centered at t_o is

$$E_{\Delta t} = \frac{1}{2}\int_{t_o - \frac{\Delta t}{2}}^{t_o + \frac{\Delta t}{2}} |\underline{f}(t)|^2 dt = \frac{1}{2}\int_{t_o - \frac{\Delta t}{2}}^{t_o + \frac{\Delta t}{2}} \int_{-\infty}^{\infty} \underline{\in}(t,\nu) d\nu dt \ . \qquad (40)$$

We can now generalize these results by determining the effect of integrating $\underline{\in}(t,\nu)$ over a finite region of the time-frequency domain [ACKROYD, 1971]. Consider the quantity $\underline{E}_{tf}$ defined by

$$\underline{E}_{tf} = \frac{1}{2}\int_{-\infty}^{\infty}\int \underline{w}_{tf}(t,\nu)\,\underline{\in}(t,\nu) dt d\nu \ , \qquad (41)$$

where $\underline{w}_{tf}(t,\nu)$ represents a two-dimensional window function in the time-frequency plane. In general we are interested only in window functions that are separable in time and frequency, and let

$$\underline{w}_{tf}(t,\nu) = \underline{w}_t(t)\underline{W}_f^*(\nu) \ . \qquad (42)$$

$\underline{E}_{tf}$ is then given by

$$\underline{E}_{tf} = \frac{1}{2}\int_{-\infty}^{\infty}\int \underline{w}_t(t)\underline{W}_f^*(\nu)\underline{f}(t)\underline{F}^*(\nu)e^{-i2\pi\nu t} d\nu dt$$

$$= \frac{1}{2}\int_{-\infty}^{\infty} \underline{w}_t(t)\underline{f}(t)\left[\int_{-\infty}^{\infty} \underline{W}_f^*(\nu)\underline{F}^*(\nu)e^{-i2\pi\nu t} d\nu\right] dt$$

$$= \frac{1}{2}\int_{-\infty}^{\infty} \underline{f}_t(t)\underline{f}_f^*(t) dt \ , \qquad (43)$$

where

$$\underline{f}_t(t) = \underline{w}_t(t)\underline{f}(t) \qquad (44)$$

and

$$\underline{f}_f(t) = \int_{-\infty}^{\infty} \underline{W}_f(\nu)\underline{F}(\nu)e^{i2\pi\nu t} d\nu \ . \qquad (45)$$

$\underline{f}_t(t)$ and $\underline{f}_f(t)$ are seen to be time-windowed and filtered versions of $\underline{f}(t)$, respectively, and $\underline{E}_{tf}$ is thus the mutual or cross energy in $\underline{f}_t(t)$ and $\underline{f}_f(t)$. By the power theorem of the Fourier theory, $\underline{E}_{tf}$ is also seen to be given by

$$\underline{E}_{tf} = \frac{1}{2}\int_{-\infty}^{\infty} \underline{F}_t(\nu)\underline{F}_f^*(\nu)d\nu \ , \tag{46}$$

where

$$\underline{F}_t(\nu) = \int_{-\infty}^{\infty} \underline{f}(t)\underline{w}_t(t)e^{-i2\pi\nu t}{}_{\nu t} \tag{47}$$

and

$$\underline{F}_f(\nu) = \underline{W}_f(\nu)\underline{F}(\nu) \quad . \tag{48}$$

As suggested by the underbar, $\underline{E}_{tf}$ is complex, consistent with the complex representation $\underline{f}(t)$ for the actual signal waveform. The real part of $\underline{E}_{tf}$ is what would be obtained if the real time-windowed and filtered functions, $f_t(t)$ and $f_f(f)$, were multiplied and the area of their product calculated. This calculation represents a symmetric midground between two other possible computations: the first where we filter, then look at the energy in the filtered function in the interval Δt; the second where the window in time, then look at the frequency domain energy in the interval Δf. Note that the three calculations yield different results, for in filtering the function we change its time characteristics (spread it out); in windowing the function we smooth its spectral characteristics. The symmetrical formulation alone prevents interaction of the time and frequency domain windowing operations.

There is a close correspondence between the computation of $\underline{E}_{tf}$ represented by Eqs. (43) and (46) and the operation performed by the variable resolution-frequency mapping spectrum analyzer of Fig. 7.

Assume the film strip input to that system moves in the negative x direction with velocity v. The resulting amplitude transmittance of the film is then $f(x+vt)$, where $f(x)$ is the spatial representation of the original signal waveform. In the following expressions we replace the real function $f(x)$ with its complex signal representation, $\underline{f}(x)$, noting that so far as output-plane distributions are concerned the input recording could contain only positive frequency components and we would not know the difference: the mapping slit operates only on the positive frequency spectral components. From Eq. (28), the output amplitude is given by

$$u_3(0,y) = \int_{-\infty}^{\infty} \underline{f}(\xi + vt)\underline{w}(\xi,y)e^{-i2\pi h(y)\xi}d\xi \ . \tag{49}$$

$\underline{w}(\xi,y)$ is the equivalent input plane window function given by $w_t(\xi,y)w_f(-\xi,y)$, as defined in Eq. (29). In order to keep our analysis as uncomplicated as possible, we assume both t and y fixed and let

$$\begin{aligned} vt &= vt_o = x_o \ , \\ h(y) &= h(y_o) = \nu_o \ , \\ w(x,y_o) &= w(x) \ , \\ W(\nu,y_o) &= W(\nu) \ . \end{aligned} \tag{50}$$

Making these substitutions and letting $\xi + vt = \xi + x_o = x$ in Eq. (49), we obtain the equivalent expression

$$u_3(0,y_o) = \int_{-\infty}^{\infty} \underline{f}(x)\underline{w}(x - x_o)e^{-i2\pi\nu_o(x - x_o)}dx \ , \tag{51}$$

where $\underline{w}(x - x_o)$ is understood to mean $\underline{w}(x - x_o,y_o)$. Using the convolution theorem, we can rewrite Eq. (51) as

$$u_3(0,y_o) = \int_{-\infty}^{\infty} \underline{F}(\nu)\underline{W}(\nu_o - \nu)e^{i2\pi x_o \nu} d\nu \ , \tag{52}$$

where

$$\underline{W}(\nu) = \mathcal{F}_x\{\underline{w}(x)\} \tag{53}$$

is likewise understood to mean $\underline{W}(\nu,y_o)$. Of ultimate interest to us is the output irradiance distribution along the y-axis, given by (for $y = y_o$)

$$I_3(0,y_o) = u_3(0,y_o)u_3^*(0,y_o) \ . \tag{54}$$

In evaluating this expression, we use Eq. (51) for $u_3(0,y_o)$ and the complex conjugate of Eq. (52) for $u_3^*(0,y_o)$, with the result

$$I_3(0,y_o) = \int_{-\infty}^{\infty}\int \underline{f}(x)\underline{w}(x - x_o)e^{-i2\pi\nu_o(x - x_o)}$$

$$\cdot \ \underline{F}^*(\nu)\underline{W}^*(\nu_o - \nu)e^{-i2\pi x_o \nu} d\nu dx \ . \tag{55}$$

With some rearrangement of terms, this can be written in the form

$$I_3(0,y_o) = \int_{-\infty}^{\infty}\int \left[\underline{f}(x)\underline{F}^*(\nu)e^{-i2\pi\nu x}\right] \tag{56}$$

$$\cdot \left[\underline{w}(x - x_o)\underline{W}^*(\nu_o - \nu)e^{-i2\pi(\nu_o - \nu)(x - x_o)}\right] d\nu dx \ .$$

The first term in brackets we recognize as the time-frequency energy density for the function f, $\underline{\mathcal{E}}_f(x,\nu)$. The remaining term plays the role of a time-frequency window function, as used in Eq. (41) for $\underline{E}_{tf}$; i.e.,

$$\underline{w}_{tf}(x,\nu) = \underline{w}(x - x_o)\underline{W}^*(\nu_o - \nu)e^{-i2\pi(\nu_o - \nu)(x - x_o)} \ . \tag{57}$$

with this identification, $I_3(0,y_o)$ is seen to be a measure of the input signal energy in that region of the time-frequency plane specified by $\underline{w}_{tf}(x,\nu)$; i.e.,

$$I_3(0,y_o) = \int_{-\infty}^{\infty}\int \underline{w}_{tf}(x,\nu)\underline{\epsilon}_f(x,\nu)dxd\nu \ , \tag{58}$$

where $\underline{w}_{tf}(x,\nu)$ is given by Eq. (57), and through Eqs. (29) and (50) is related to the equivalent input plane window function. For an alternative representation, note that the quantity $\underline{w}(x - x_o)\underline{W}^*(\nu_o - \nu)e^{-i2\pi(\nu_o - \nu)(x - x_o)}$ is itself in the form of a signal energy density function. Specifically, let

$$\underline{\epsilon}_w(x,\nu) = \underline{w}(x)\underline{W}^*(\nu)e^{-i2\pi\nu x} \ . \tag{59}$$

Then $\underline{w}_{tf}(x,\nu) = \underline{\epsilon}_w(x - x_o, \nu_o - \nu)$,

and

$$I(0,y_o) = \int_{-\infty}^{\infty}\int \underline{\epsilon}_f(x,\nu)\underline{\epsilon}_w(x - x_o, \nu_o - \nu)dxd\nu \ . \tag{60}$$

If we let $\underline{\tilde{\epsilon}}_w(x,\nu) = \underline{\epsilon}_w(-x,\nu)$,

then

$$I(0,y_o) = \int_{-\infty}^{\infty}\int \underline{\epsilon}_f(x,\nu)\underline{\tilde{\epsilon}}_w(x_o - x, \nu_o - \nu)dxd\nu \ , \tag{61}$$

which we recognize to be the two-dimensional convolution of $\underline{\epsilon}_f(x_o,\nu_o)$ and the time-reversed version of $\underline{\epsilon}_w(x_o,\nu_o)$.

IV. FREQUENCY-VARIANT SIGNAL WAVEFORM PROCESSING

Spectrum analysis is a form of signal processing, and the operations described in Section II are thus justifiably described as two-dimensional processing operations on one-dimensional signals. Signal processing often implys more than a display of signal properties as output, however. In this section we describe an optical system that has a signal waveform for its output as well as for its input. This system, also requiring two degrees of freedom for its operation, exemplifies in the most general sense two-dimensional processing of a one-dimensional signal.

The heart of the operation is a mapping--similar to the logarithmic mapping of the log-frequency spectrum analyzer of Section II--of frequency components of the short-time amplitude spectrum of the signal waveform to new locations in the frequency diagram. The mapping is initially one of spatial frequency components of the signal as presented in the optical system but is converted to a mapping of temporal frequency components by an optical heterodyne technique. The basic system employed is similar in many respects to a system described by WHITMAN, KORPEL, and LOTSOFF for use in simulating the amplitude and phase characteristics of electrical networks. In their system, illustrated in Fig. 12, a Bragg cell, which serves to produce a moving signal transparency in real time, is used to convert the frequency spread of an RF signal into a spatial spread of light frequencies on the surface of an optical square-law detector. For a sinusoidal input signal of frequency ν_s, the optical frequency of the diffracted beam is shifted from laser frequency ν_o to $\nu_o + \nu_s$. This diffracted beam is focused at position x, x proportional to ν_s, on the photo-multiplier tube (the square-law detector), where it mixes with a coherent local-oscillator wave at laser frequency ν_o. An electrical signal at the original rf frequency is recovered. Superposition can be applied for a spread of frequencies present in the input. The relative phase and amplitude of the various recovered rf frequencies depend on the relative phase and amplitude of the local oscillator field at the associated values of x. These parameters can in turn be controlled by suitable choice of the optical system that determines the local oscillator field.

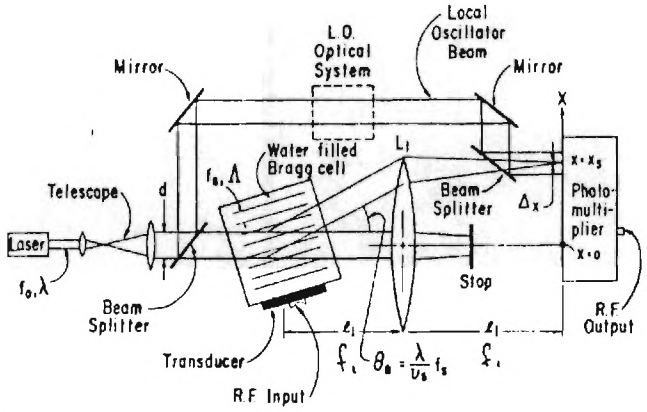

Fig. 12. Zenith system for signal processing. Optical frequency of diffracted beam is shifted from laser frequency, f_o, to f_o+f_s by frequency of rf input signal. This diffracted beam is focused at position x, where x is proportional to f_s, on the photo-multiplier tube (square-law detector), where it mixes with a coherent local-oscillator wave at laser frequency f_o. An electrical signal at the original rf frequency is recovered. Superposition can be applied for a spread of frequencies present in the input. The relative phase and amplitude of the various recovered rf frequencies depend on the relative phase and amplitude of the local oscillator field at the associated values of x. These parameters can in turn be controlled by suitable choice of the "optical system" that determines the local oscillator field [after WHITMAN, KORPEL, and LOTSOFF].

Our own system, illustrated schematically in Fig. 13, differs from the above system primarily in the application of frequency-variant windowing to the input signal and in the non-linear mappings of the input signal frequencies into output signal frequencies. The system designer has great flexibility in determining how windowing and nonlinear mappings will be accomplished. We consider here a particular system configuration based the variable resolution-frequency mapping spectrum analyzer of Section II. The signal optics portion of the processing system can, in fact, be identical to the system illustrated in Fig. 7. The output, incident on the photomultiplier tube, is a distribution of light showing the local spectral content of the input signal vs. an arbitrary monatonic function of frequency and with frequency-varying spectral resolution. As before, the optical frequency of the signal arm distribution on the PMT varies as a function of spatial position; however, the frequency vs. position function need no longer be linear. Superposed on this distribution is the output of the local oscillator optical system. This system performs a conventional (i.e., non-frequency variant) spectral analysis on the local oscillator input signal, whose characteristics we discuss shortly, and the optical frequency of the local oscillator distribution on the PMT thus varies linearly with position. In Fig. 14(a) we have plotted exemplary optical frequency vs. distance curves for the two superposed distributions, temporarily ignoring the finite limits on spectral resolution imposed by various masks in the systems. The result of the square-law detection at the PMT is a heterodyne translation of the frequencies of the input signal in accord with the difference in optical frequencies of the two distributions as a function of position on the detector. A curve representing

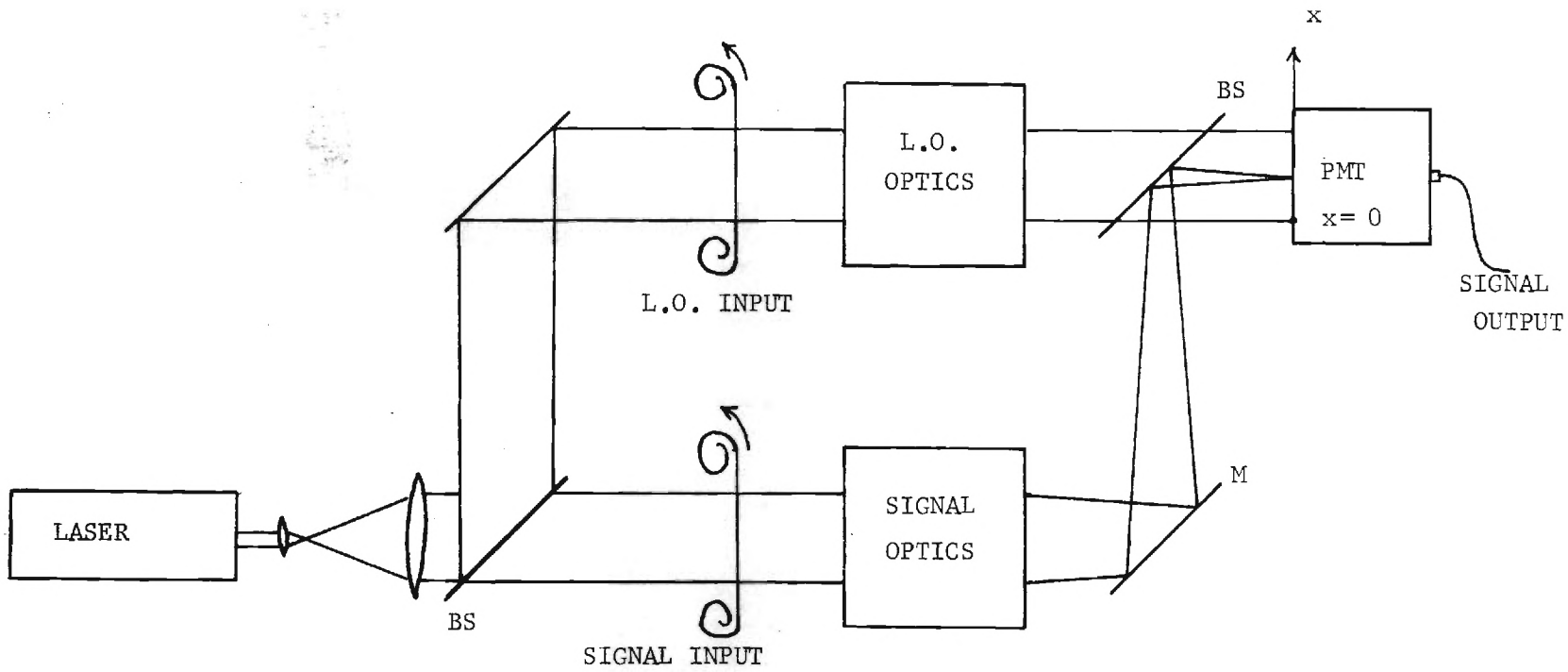

Fig. 13. Bandwidth compression system. Signal-optics section performs spectral analysis on moving input recording with frequency-dependent window length. Position x and optical frequency shift of focused output beam is proportional to input signal frequency. Local-oscillator-beam optics generate local oscillator light distribution at photomultiplier tube with optical frequency varying nonlinearly with x. Square-law detection produces output signal at the difference frequency $\nu_{LO}(x) - \nu_{sig}(x)$.

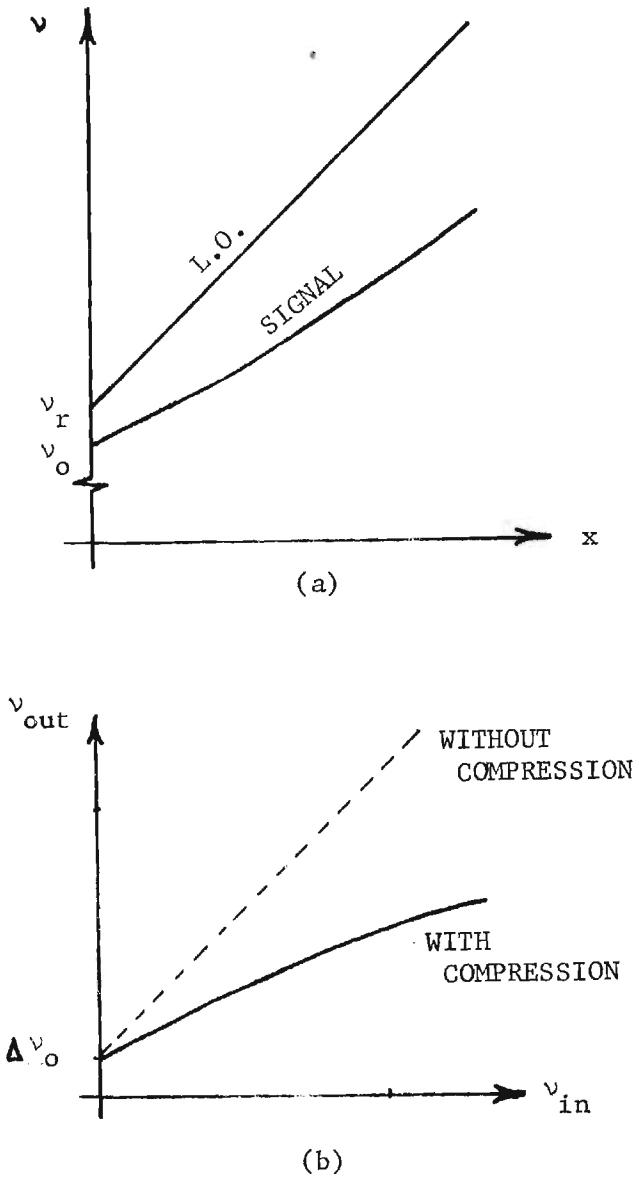

Fig. 14. Operation of frequency mapping signal waveform processor. Optical frequency of signal spectrum distribution increases nonlinearly with x, in contrast to that of signal spectrum distribution, (a). Heterodyne operation at detector shifts input signal frequencies according to nonlinear compression curve, (b). Frequency offset allows filtering of intermodulation components.

the resultant frequency compression is shown in Fig. 14(b). The offset frequency shown, $\Delta\nu_o$, must be provided for in the system: because of finite spectral resolution, signal spectral components sufficiently close together will produce low-frequency beat tones, or intermodulation products, by the homodyning of the signal spectrum distribution with itself. These intermodulation products will have an upper cutoff frequency, however, determined by the optical system. By choosing $\Delta\nu_o$ sufficiently high, the desired compressed-frequency signal waveform can be separated from the beat-generated noise by high-pass filtering.

The specific characteristics of the resultant output signal depend upon the design of the signal optics and local oscillator optics and on the characteristics of the local oscillator input signal. These systems are currently under study and detailed comments are reserved for a later report. However, basic system capabilities are suggested by the diagramatic representation in Fig. 15. In this figure, $f_{in}(t)$ and $f_{out}(t)$ are complex signal representations for the input and output signals. The nature of the optical system is such that the bandpass filtering and frequency shifting operations performed can be either channelized, as shown in the figure, or continuous in frequency. In a channelized version, the number of individual bandpass filter-local oscillator stages can range from one or two up to a number imposed by the one-dimensional space-bandwidth product of the optical system--somewhere between 10^3 and 10^4, depending on optical components. Choice of local oscillator frequencies and filter characteristics is quite flexible, particularly when the amplitude and phase modifying capabilities of recently developed computer holograms are considered [CHU, FEINUP,

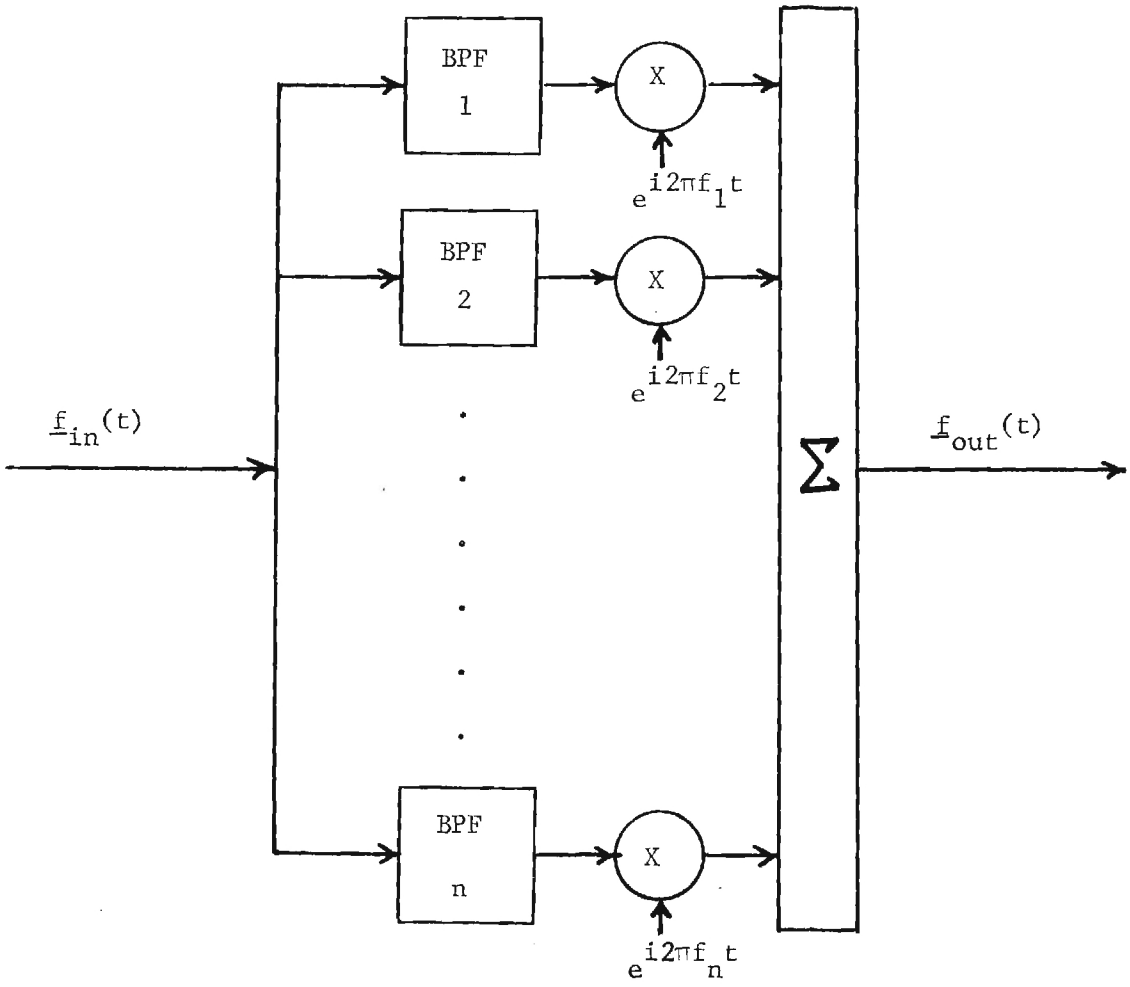

Fig. 15. Schematic representation of (channelized) frequency variant-frequency shifting operation performed by optical system. Center frequencies and bandwidths of bandpass filters (BPF's) can be chosen arbitrarily.

GOODMAN]. If desired, the local oscillator signals can be narrowband noise waveforms rather than discrete-frequency sinusoids. A more appropriate representation of the system is, in fact, that of Fig. 16, where input and local oscillator signals are treated in the same manner. The signal processing operations performed by such a system can be performed by conventional electronic systems, but not on the scale (10^3 to 10^4 separate channels) afforded by the optical system.

Frequency-variant signal processing systems of this kind appear to have potential applicability in such areas as bandwidth compression and re-expansion of video and radar signals and in the variable-rate playback processing of audio signals, where a compression or expansion of the signal time base must be accompanied by a corresponding compression or expansion of the signal bandwidth to preserve original pitch characteristics. When compared to the conventionally employed techniques for such signal processing [GABOR; FAIRBANKS et al.; KOCH; SCHIFFMAN], the two-dimensional approach appears to offer significant advantages. Further research will tell.

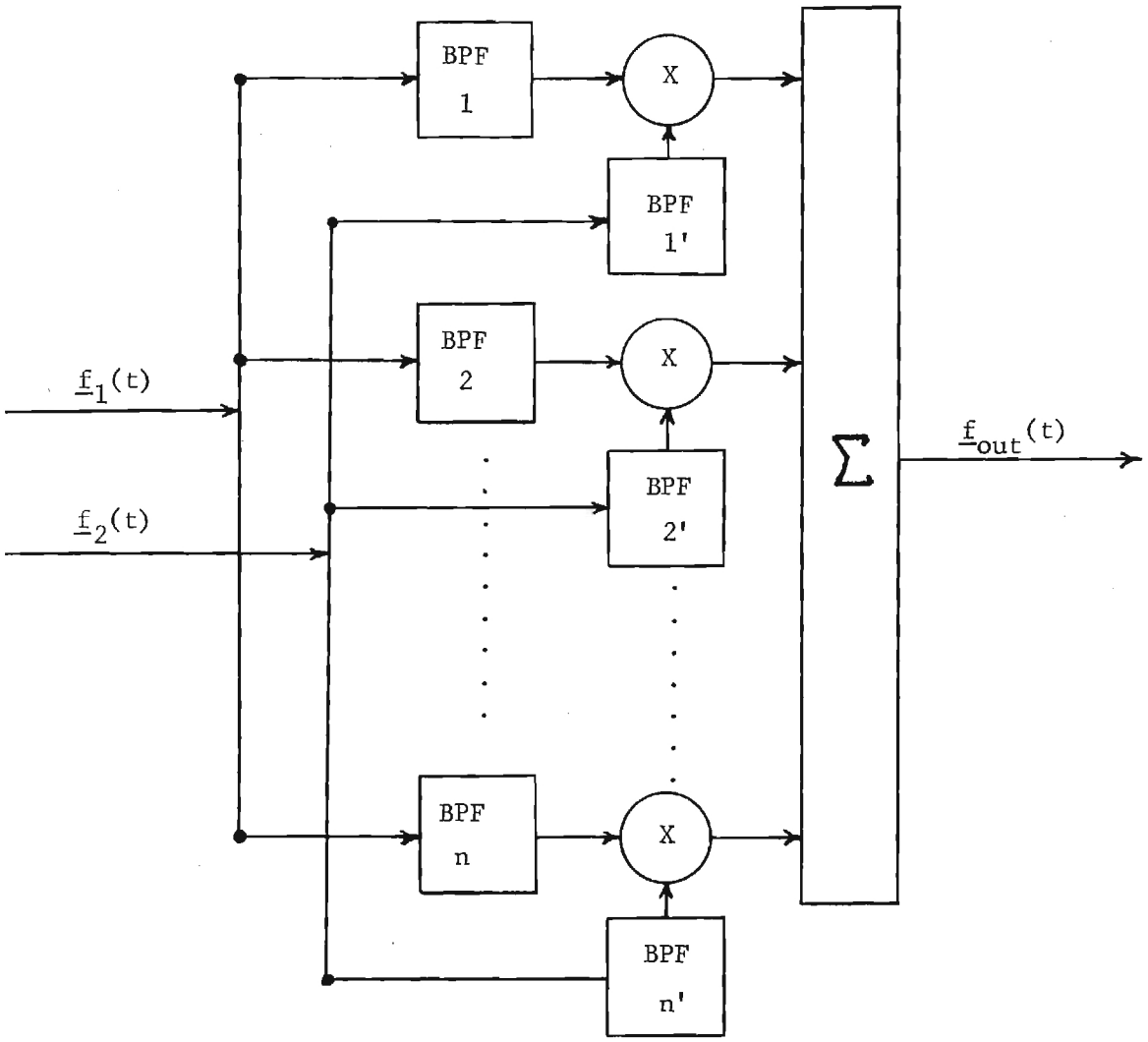

Fig. 16. Schematic representation of general channelized operation performed by frequency variant-frequency shifting signal waveform processing system.

V. CONCLUDING REMARKS AND ACKNOWLEDGMENTS

It is often interesting to delve into the background and sources of inspiration for a research project. In the case of the research reported here, the source of much early inspiration was work done by Dennis Gabor in the middle 1940's, several years before he developed the principle of holography. In the interest of historical continuity, a brief description of certain aspects of Gabor's work and their relationship to this project are presented in Appendix B.

We want to express our appreciation to Olof Bryngdahl for providing us with additional insight into the nature of space- and frequency-variant optical systems and to Art Korpel for some excellent advice regarding the construction of our own optical systems. Above all, we want to thank Leonard Laub for numerous discussions of great importance to this work. Without his contributions we could not have come nearly so far so fast. Special thanks go to the National Science Foundation for their generous support of this research.

APPENDIX A

LOG-FREQUENCY SPECTRUM ANALYZER USING A HOLOGRAPHIC MAPPING ELEMENT

The system shown in Fig. A-1 has as its output a log-frequency display of the input signal spectral content, just as does the system of Fig. 5; however, the system discussed here performs the log-frequency mapping using a holographic mapping element rather than a slit mapping element. As in analyzing the slit mapping system, we assume the input transparency, shown in Fig. A-2(a), to be a recording of sinusoids with frequencies in the proportions 1:2:4:8.

Lens combination L_2, L_3, L_4 images the input transparency in the vertical (across-signal) direction, Fourier transforming it in the horizontal direction. (The negative cylindrical lens L_4 serves to remove a quadratic phase factor across plane P_2. The lens can be eliminated if the proper cylindrical phase factor is incorporated into the mapping element that follows.) The resulting distribution in plane P_2 is shown in Fig. A-2(b). In plane P_2 is placed a special optical element that behaves much like a prism, but one whose wedge-angle increases logarithmically with horizontal distance from the origin. Analytically, the element is represented by the light-amplitude transmittance function

$$t(\nu,y) = \begin{cases} \exp\{j[(y-y_o)\log \nu]\}, & \nu_1 \leq \nu \leq \nu_2,\ -y_o \leq y \leq y_o, \\ 0 & \text{otherwise,} \end{cases}$$

where the horizontal coordinate is associated with the temporal frequency, ν, of the input signal. The non-zero portion of this transmittance

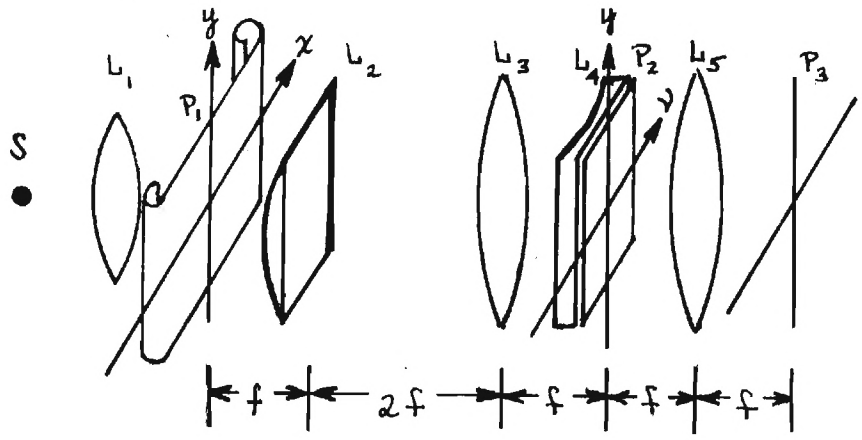

Fig. A-1. Log-frequency optical spectrum analyzer using holographic mapping element. Input signal recording at P_1 is imaged onto P_2 in y direction and Fourier transformed in x direction by lens combination L_2, L_3, L_4 (L_4 serves to remove a quadratic phase factor across P_2). Special optical element, usually holographic, at P_2 introduces wavefront tilt in y direction that increases as $\ln(\nu)$. Lens L_5 Fourier transforms modified amplitude distribution, with the desired log-frequency spectral display appearing along the vertical axis at P_3.

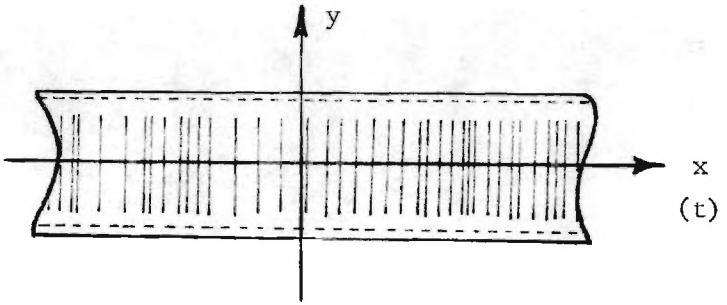

(a)

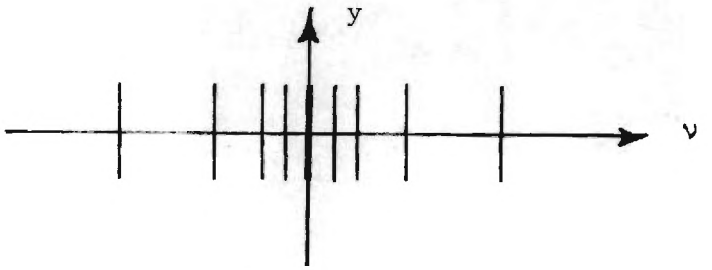

(b)

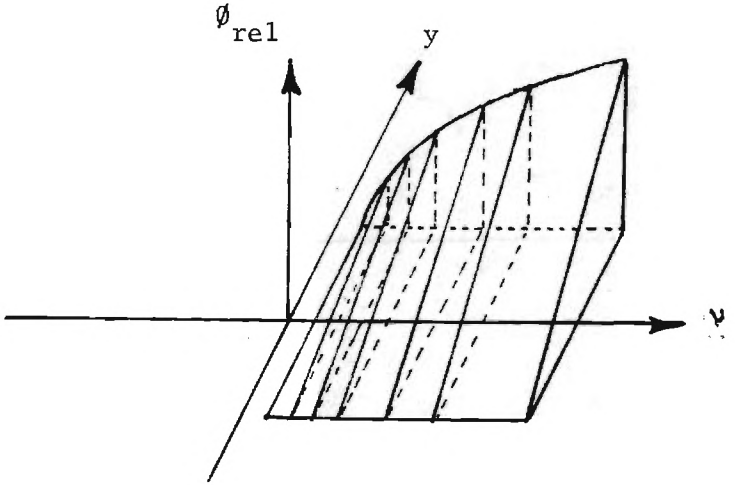

(c)

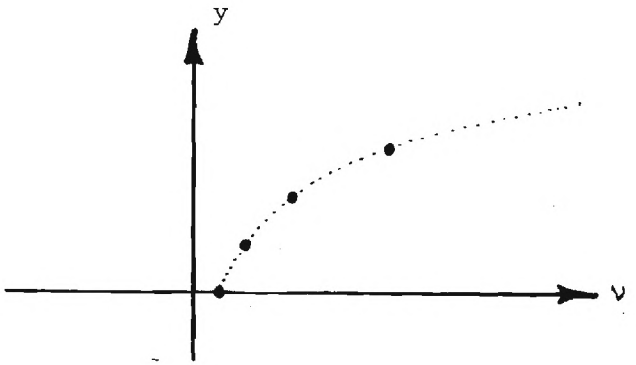

(d)

(e)

Fig. A-2. Log-frequency display holographic mapping optical spectrum analyzer: intermediate stages. Input transparency (a) is Fourier transformed in x direction, imaged in y direction. Sinusoidal components at 1, 2, 4, and 8 cycles per unit time are displayed in (b). Relative phase function of transparent portion of optical element is shown in (c). After modification by optical element, vertical Fourier transform yields distribution in (d); accompanying transform in horizontal direction yields, along vertical axis, distribution shown in (e).

function, which can be effected either with a specially-fabricated glass element or with a holographic optical element, is illustrated in Fig. A-2(c).

The effect of this element in the system is most easily understood if we treat the final two-dimensional Fourier transform operation, performed by spherical lens L_5 in Fig. A-1, as a vertical transform-horizontal imaging operation followed by a horizontal transform-vertical imaging operation. The vertical transform collapses the line amplitude distributions of Fig. A-2(b), which represent spectral components of the input transparency, down to diffraction-limited spots. Because of the special optical element in plane P_2, however, these spots appear not along a horizontal line, but along a logarithmic curve, as shown in Fig. A-2(d). The subsequent horizontal transform converts each such spot of light, at its original vertical displacement from the origin, into a smear about the vertical axis. Since the light amplitude along this vertical line is proportional to the zero spatial frequency component in the horizontal direction for each vertical displacement, masking off all but a narrow region about the line (and introducing a $1/\nu$ amplitude attentuation to compensate for greater spot-packing with larger values of ν) results in an amplitude distribution, shown in Fig. A-2(e), that displays the spectral content of the input signal as a function of log (ν). These two transform operations are, of course, performed simultaneously by the single spherical lens, L_5. By adjusting various parameters in the system, it is possible to change the scale of the final output display. It is, in fact, possible to display signal spectral content vs. any real-valued function of frequency simply by changing the functional form of the exponent in the transmittance function $t(\nu,y)$. A general analysis

follows. Proportionality constants are ignored and all distributions are assumed infinite in extent for simplicity in the resulting expressions.

If temporal function f(t) is mapped into spatial function f(x) by the signal recording process, then the input transparency gives rise to a light-amplitude distribution at P_1 of Fig. A-1 containing the term

$$u_1(x,y) = f(x) \ . \tag{A.1}$$

Transforming in x (with $x \rightarrow \nu$ under the transformation) and imaging in y, we obtain at P_2 the distribution

$$u_2(\nu,y) = F(\nu) \ , \tag{A.2}$$

where

$$F(\nu) = \int_{-\infty}^{\infty} f(t)e^{-i2\pi\nu t} \ .$$

The transmittance function of the special optical element can be expressed in the general form

$$t(\nu,y) = \exp[i2\pi g(\nu)y] \ , \tag{A.3}$$

where $g(\nu)$ is considered here a real-valued function of ν. The distribution at P_2, after modification by this optical element, is

$$u_2(\nu,y) = F(\nu)e^{i2\pi g(\nu)y} \ . \tag{A.4}$$

Along the vertical axis in the output plane, the light-amplitude distribution, u_3, is given by the expression

$$u_3(0,\eta) = \int_{-\infty}^{\infty}\int u_2(\nu,y)e^{-i2\pi(\nu\xi + y\eta)}d\nu dy\Big|_{\xi = 0} \tag{A.5}$$

$$= \int_{-\infty}^{\infty} d\nu F(\nu) \int_{-\infty}^{\infty} e^{-i2\pi[\eta - g(\nu)]y} dy$$

$$= \int_{-\infty}^{\infty} d\nu F(\nu)\delta(\eta - g(\nu)) \ . \tag{A.6}$$

By using the relationship*

$$\delta[f(x)] = \sum_n \frac{\delta(x - x_n)}{|f'(x_n)|} \ ,$$

where x_n are the roots of $f(x) = 0$ (and $f'(x_n)$ exists and is not zero), we can evaluate Eq. (A.6), with the result

$$u_3(0,y) = \frac{1}{|g'(\nu)|} F(\nu) \ , \tag{A.7}$$

where

$$y = g(\nu) \ .$$

Alternatively, we have

$$u_3(0,y) = \frac{1}{|g'(g^{-1}(y))|} F(g^{-1}(y)) ,$$

where

$$g^{-1}(y) = \nu \ .$$

As suggested earlier, the optical element that performs the spectral component mapping operation can be made holographically. In that case the transmittance function, Eq. (A.3), becomes

$$t(\nu,y) = 1 + m \cos[2\pi(g_o + g(\nu))y] \ , \tag{A.8}$$

---

*R. N. Bracewell, The Fourier Transform and Its Applications, McGraw-Hill, 1965, p. 95

where g_o represents an offset carrier frequency. Fig. A-3 shows the appearance of such a holographic mapping element. The recording process is basically quite simple. As illustrated in Fig. A-4, the desired mapping curve, $g(\cdot)$, is plotted on white paper above a horizontal line, which serves as a line impulse reference. A high-contrast negative photograph is made of this pattern and placed in the input plane of a system that images in the horizontal direction and Fourier transforms in the vertical direction. The resultant distribution in the output plane consists of a space-varying sinusoidal fringe pattern like that of Fig. A-3, which is recorded on high resolution film. The recording can be of high contrast for improved diffraction efficiency when used in the spectrm analyzer. To avoid confusion resulting from multiple diffraction orders, the distance b in Fig. A-4 must then be no larger than twice the offset distance a.

Figure A-5 shows the output of a holographic mapping element log-frequency spectrum analyzer when the input contains four logarithmically spaced frequency components. Octaves are now represented by equal distances in the output plane display. The double-image appearance of the output is a natural consequence of the holographic mapping process.

The holographic mapping technique appears to offer no significant advantages over the slit mapping technique discussed in the body of the report, other than a possible improvement in light utilization efficiency. The holographic element uses light from the entire intermediate plane of the optical system, whereas the slit mapping technique uses only the light that passes the slit. The holographic technique lacks versatility, however, in that it cannot be used with a non-uniform input window for, as an example, combined log frequency-constant Q spectral analysis.

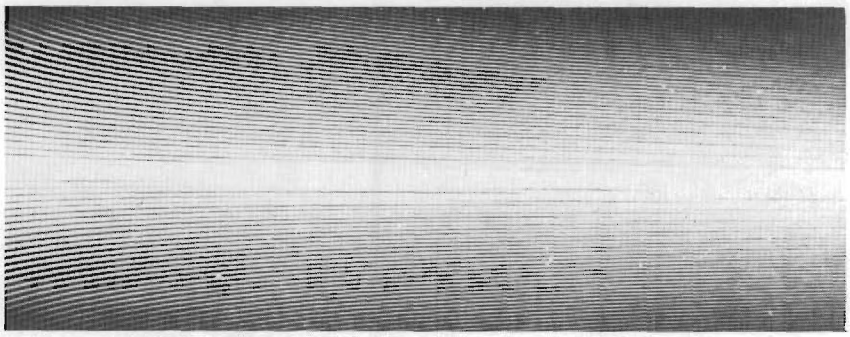

Fig. A-3. Log-frequency holographic mapping element.

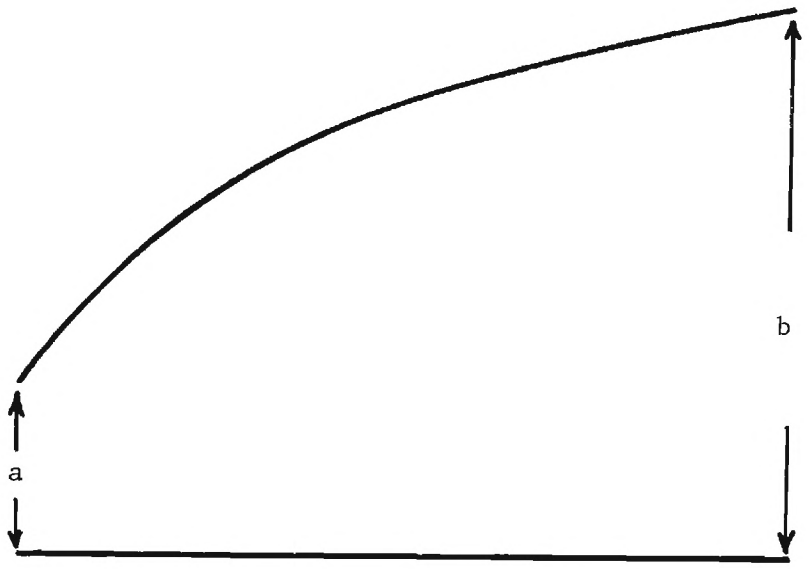

Fig. A-4. Mapping curve and straight line reference used to record holographic mapping element. To avoid problems with higher order diffraction terms, should have $b > 3a$; with careful exposure, $b > 2a$ sufficient.

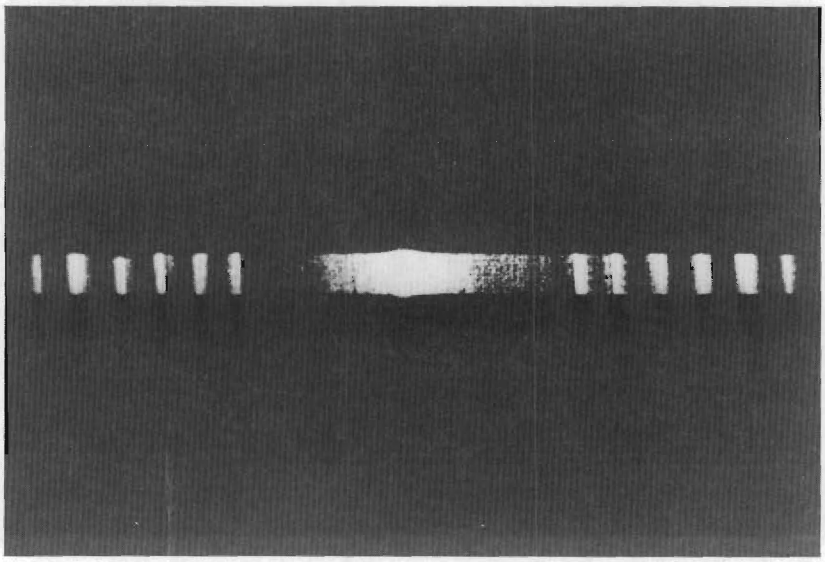

Fig. A-5. Output of holographic mapping log-frequency spectrum analyzer. Input consisted of four logarithmically spaced frequency components.

APPENDIX B

HISTORICAL BACKGROUND FOR RESEARCH EFFORT

In 1946, Dennis Gabor published a paper in which he noted that the ability of the human ear to discriminate between fundamental quanta of sound information (sound packets of minimum time-frequency uncertainty product) is, as shown in Fig. B-1, approximately one-half that of an ideal sound-detecting instrument in the frequency range 60-1000 Hz and falls off above that frequency to about 15% at 8000 Hz. Gabor concluded that, as a consequence of these characteristics, "'condensed' methods of transmission and reproduction [of speech or music] with improved waveband economy are possible in principle" [GABOR]. He proceeded to show that such bandwidth economy in speech transmission was indeed possible by demonstrating, analytically and experimentally, methods of proportionally compressing and subsequently expanding the frequency content of a speech pattern--without increasing the time necessary for message transmission--in such a way that the ear was largely unaware of the process.*

---

*Gabor's work in audio signal bandwidth compression was preceded by several years by Homer Dudley's development at Bell Labs of the Channel Vocoder [DUDLEY] and roughly paralleled by G. Fairbanks' development of what has come to be known as the "sample- and discard" or "sampling" method of time/bandwidth compression [FAIRBANKS, EVERITT, and JAEGER]. Today, the Gabor/Fairbanks method (the two approaches are essentially the same) is represented by several commercially-available systems [KOCH; LEXICON, INC.; DISCERNED SOUND], and a recent offspring of the original channel vocoder is being considered for use in government communication applications. During the past decade, additional more effective techniques have been developed for reducing data rates in speech communications systems, including homomorphic [OPPENHEIM; OPPENHEIM and SCHAFER] and linear-predictive [ATAL and HANAUER] vocoder techniques. It should be noted that these latter vocoder techniques are in general not suited to reducing data rates for arbitrary audio signals.

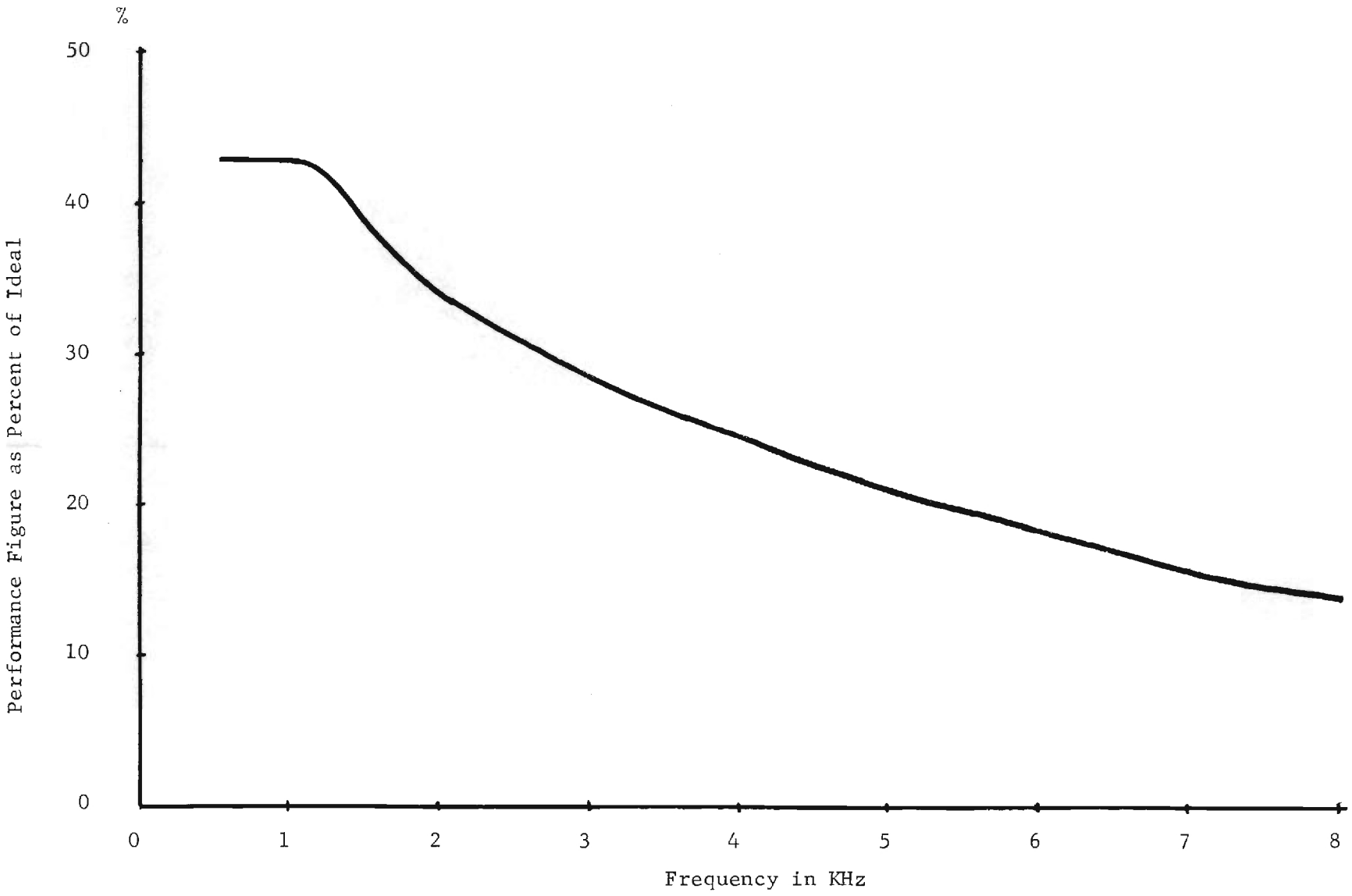

Fig. B-1 Performance figure of the ear as sound-information detecting instrument. The performance of the ear is nearly ideal (50%) for a phase-insensitive detector in the 60-1000 Hz range. Above about 1000 Hz, the hearing mechanism changes and performance falls off.

A system proposed by Gabor for performing such a compression-expansion operation is shown in Fig. B-2. Quoting his original paper [GABOR, pp. 445-446]:

> Assume that the message to be condensed or expanded is recorded as a sound track on a film. For simplicity, assume that the original signal is a simple harmonic oscillation, that is to say, a frequency f_o--to be called the "original frequency"--is produced if the record moves with standard speed v past a stationary slit. Imagine now that the slit itself is moving with some speed u, so that its speed relative to the film is v-u. The photocell behind the film now collects fluctuations of light of frequency
>
> $$f_1 = \frac{v-u}{v_o} f_o \quad .$$
>
> This means that all frequencies in the record are converted in a constant ratio (v-u)/v. There is evidently no gain, as it would take the moving slit v/(v-u) times longer to explore a certain length of the film than if it were stationary. But let us now imagine that the film moves across a fixed window, so that the moving slit is effective only during the time in which it traverses the window. In order to get a continuous record let a second slit appear at or before the instant at which the first slit moves out of the window, after which a third slit would appear, and so on. The device is still not practicable, as evidently every slit would produce a loud crack at the instant at which it appeared before the window and when it left it. But now assume that the window has continuously graded transmission, full in the middle and fading out at both sides to total opacity. In this arrangement the slits are faded in and out gradually, so that abrupt cracks can be avoided.

This is a description of the prototype of Gabor's "kinematical" frequency converter, which he investigates in some detail.*

This method of bandwidth compression suffers from several significant drawbacks. To begin with, certain frequencies are transmitted better by

---

*In the same paper he describes alternative but equivalent systems for accomplishing the same objective, including a system appropriate for recordings on magnetic tape (differing only in details from FAIRBANKS' method) and a completely electrical system.

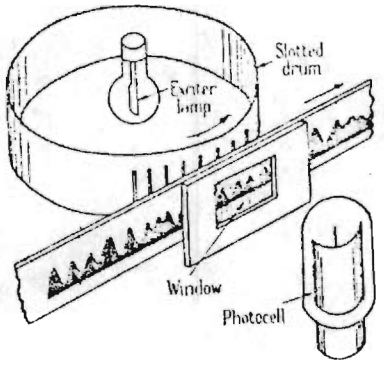

Fig. B-2 Gabor's "kinematical" frequency converter (after GABOR).

the system than others. Each slit, as it passes before the window, produces an output oscillation with frequency f_1 and gaussian envelope, as illustrated in Fig. B-3. The contributions of the individual slits produce for some frequencies a very nearly faithful reproduction of the original sinusoid, shifted in frequency. For other frequencies, however, there can be strong beats. For a window length (defined as the part of the window for which the transmittance exceeds 1/e times its maximum value) of about 30 msec, a length Gabor considers roughly optimum for speech, optimally reproduced frequencies are spaced by about 20 Hz. Between these optimally reproduced frequencies, however, are tones reproduced at a fraction of their original amplitude--down to about 0.56 under optimum conditions.

A second major drawback of the described system is the fixed window length. Some portions of a speech or music pattern require good time resolution for unambiguous interpretation, while other portions require good frequency resolution. The ear accomodates these apparently conflicting requirements through a mechanism Gabor describes as an "adjustable time-constant": the ear's time resolution sometimes approaches 10 msec, its frequency resolution sometimes approaches 4 Hz, or $(250 \text{ msec})^{-1}$. Vocoder systems (and Gabor's system comes under this heading), which for the most part respond to the momentary spectral content or short amplitude spectrum of a speech waveform, typically operate with fixed time windows of roughly 30 msec duration. Their performance suffers as a consequence of this compromise, a fact demonstrated several years ago at The Georgia Institute of Technology by the implementation of adaptive time-windowing techniques in a simulated vocoder system [HAMMETT].

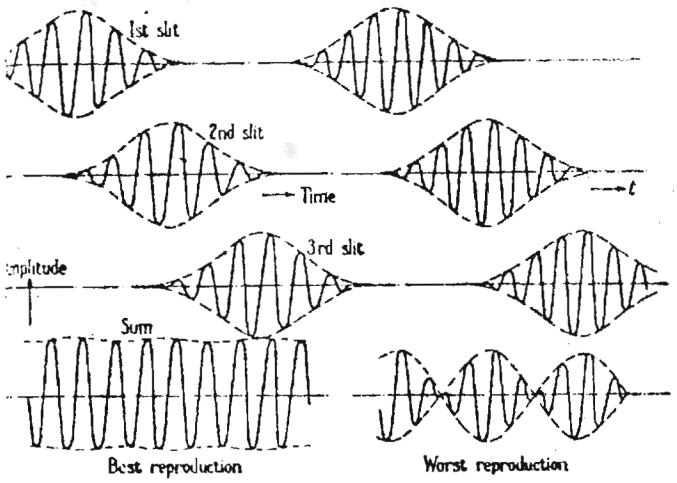

Fig. B-3. The contributions of individual slits and the resulting light output (after GABOR).

A final drawback of Gabor's system--and of any system based on his technique--is that it goes only part way in realizing the full bandwidth compression possible with such a frequency-shifting scheme. As noted in Fig. B-1, the ear's ability to utilize information is not constant with frequency. The scheme just described, however, compresses frequency components uniformly across the entire frequency band. More appropriate would be a mapping scheme that compressed high frequencies more than low frequencies, perhaps as the reciprocal of the curve in Fig. B-1. If such a nonlinear compression curve is employed, the total achievable bandwidth compression is no longer a straight-line function of frequency but a curve, as shown in Fig. B-4.* For a 0-1000 Hz signal, achievable bandwidth compression (within the limits imposed by this curve) is only about 2:1. For a 0-4000 Hz (telephone quality) signal, however, the ratio is closer to 3:1, and for a 0-8000 Hz signal, nearly 4:1. If such high bandwidth compression ratios were attempted with Gabor's system, i.e., with uniform compression across the entire bandwidth, it would be at the expense of frequency resolution in the 0-1000 Hz range--resolution that appears to be necessary for satisfactory pitch discrimination.

The two-dimensional optical signal processing approach discussed in the body of this report, with its great flexibility, provides ways of overcoming all of these difficulties, at least to a very great extent. The problem of unfaithful reproduction or beats at certain

---

*The appropriateness of non-linear bandwidth compression has been noted by a number of investigators. VILBIG [1950a,b] experimented with an optical/mechanical technique in the late 1940's and early 1950's that allowed a non-linear relocation of speech spectral components. Channel vocoders are also generally designed for greater data compression at higher frequencies than at lower; see, for example, the paper by TIERNEY et al.

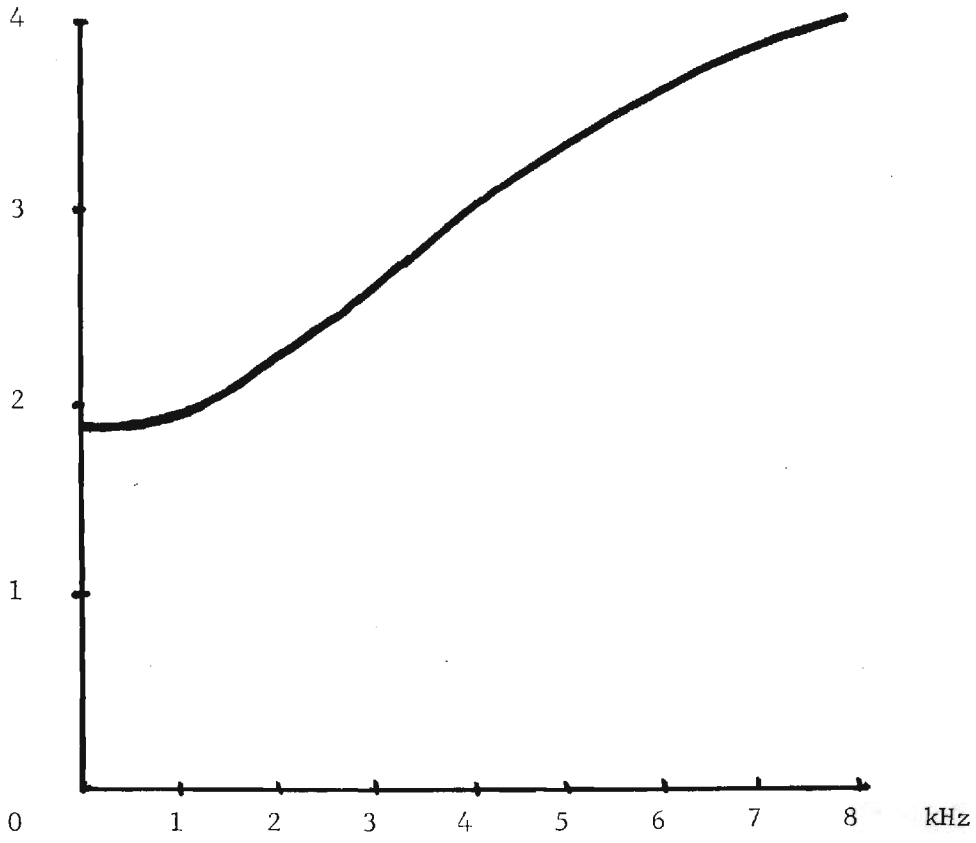

Fig. B-4 Total achievable bandwidth compression (undiscernable to the ear) with frequency-dependent compression ratio, for audio signals of different initial bandwidths, as based on Fig. B-1

frequencies, for example, can be reduced significantly by the employment of different window lengths for different frequencies. Non-linear mappings of frequency components can be accomplished using the same kind of system as employed in the log-frequency spectrum analyzer discussed earlier. Most important, perhaps, it is possible for a two-dimensional signal processor to improve on the fixed-window compromise of Gabor's and other vocoder systems. This latter statement is based on the observation that speech and music cues requiring good time resolution are generally characterized by predominant high-frequency content. Cues requiring good frequency discrimination, on the other hand, and therefore requiring a long time window, are characterized by predominant low-frequency content--in the 60-1000 Hz range. It thus appears desirable to observe the high frequency content of a signal waveform with a relatively short time window and to observe the low frequency content with a relatively long time window. Coherent optical systems related to the frequency-variant spectrum analyzers discussed in Section II of this report can perform just such an operation by employing the differential time windowing technique such that the effective time window is continuously changing as a function of frequency.

REFERENCES

Ackroyd, M. H., "Instantaneous and Time-Varying Spectra--An Introduction," The Radio and Electronic Engineer 39, 145 (1970).

_____ "Short-Time Spectra and Time-Frequency Energy Distributions," J. Acoust. Soc. Am., 50 1229 (1971).

Atal, B. S., Hanauer, S. L., "Low-bit-rate speech transmission by linear prediction of speech signals," J. Acoust Soc. Am. 49, 133(A) (1971).

_____ _____ "Speech analysis and synthesis by linear prediction of the speech waves," J. Acoust. Soc. Am. 50, 637-655 (1971).

Braccini, C., Oppenheim, A. V., "Unequal Bandwidth Spectral Analysis Using Digital Frequency Warping," IEEE Trans. ASSP-22, 236 (1974).

Bryngdahl, O., "Geometrical Transformations in Optics," J. Opt. Soc. Am. 64, 1092 (1974).

Chu, D. C., Feinup, J. R., Goodman, J. W., "Multi-Emulsion On-Axis Computer-Generated Hologram," Appl. Opt. 12, 1386 (1973).

Cutrona, L., "Recent developments in coherent optical technology," in Optical and Electro-Optical Information Processing, Tippett et al eds., MIT Press, 1965.

Discerned Sound, "The Whirling Dervish;" information available from Discerned Sound, 4459 Kraft Avenue, North Hollywood, Calif. 91602.

Dudley, H., "Remaking speech," J. Acoust. Soc. Am. 11, 169-177 (1939).

_____ "The carrier nature of speech," The Bell System Tech. Jour. 19, 495-515 (1940).

Fairbanks, G., Everitt, W. L., Jaeger, R. P., "Method for Time or Frequency Compression-Expansion of Speech," IRE Trans. Audio AU-2, 7-12 (1954).

Flanagan, J. L., Speech Analysis, Synthesis, and Perception, Springer-Verlag (New York), 1972.

Gabor, D., "Theory of Communications," J. of the IEE 93, 429-457, London (1946).

Hammett, J. C., "An Adaptive Spectrum Analysis Vocoder," Ph.D. thesis, Georgia Institute of Technology, 1971, available from University Microfilms, Ann Arbor, Michigan.

Helstrom, C. W., "An Expansion of a Signal in Gaussian Elementary Signals," IEEE Trans. on Info. Theory, Jan. 1966, pp. 81-82 (1966).

Jenkens, G. M., Watts, D. G., Spectral Analysis and Its Applications, Holden-Day Company (San Francisco), 1969.

Karkevich, A. A., "Spectra and Analysis" (translated from the Russian); (Consultants Bureau, New York, 1960).

Koch, R. F., "The Ambichron™: An Electronic Time Compressor for Audio," in the Proceedings of the 1972 Conference on Speech Communication and Processing, 24-26 April 1972, Newton, Mass., pp. 45-48 (1972).

Lerner, R. M., "The Representation of Signals," IEEE Trans. on Circuit Theory, Special Supplement, pp. 197-216, May 1959.

Lexicon, "Varispeech-I " available from Lexicon, Inc., 60 Turner Street, Waltham, Mass. 02154.

Markevitch, B. V., "Optical processing of wideband signals," in "Five Ampex Corporation Papers Presented at the Third Wideband Analog Recording Symposium, Rome Air Development Center, Griffiss AFB, New York, Sept. 1969."

Montgomery, L. K., Jr., Reed, I. S., "A Generalization of the Gabor-Helstrom Transform," IEEE Trans. on Info. Theory, April 1967, pp. 344-345 (1967).

Oppenheim, A. V., "Speech analysis-synthesis system based on homomorphic filtering," J. Acoust. Soc. Am. 45, 459-462 (1969).

_____ Schafer, R. W., "Homomorphic analysis of speech," IEEE Trans. Audio and Electroacoust. AU-16, 221-226 (1968).

Papoulis, A., Systems and Transforms with Applications in Optics, McGraw-Hill (New York), 1968.

_____ "Apodization for Optimum Imaging of Smooth Objects," J. Opt. Soc. Am. 62, 1423 (1972).

_____ "Minimum-Bias Windows for High-Resolution Spectral Estimates," IEEE Trans. IT-19, 9 (1973).

Rhodes, W. T., "New Approach to Optical Processing of One-Dimensional Signals," (A), J. Opt. Soc. Am. 64, 545 (1974).

_____ Limburg, W. R., "Coherent and non-coherent optical processing of analog signals," in Proceedings of the 1972 Electro-Optical Systems Design Conference, 12-14 September 1972, New York, pp. 314-320 (1972).

Rihaczek, A. W., "Signal Energy Distribution in Time and Frequency," IEEE Trans. IT-14, 369, (1968).

Schiffman, M., "Playback Control Speeds or Slows Taped Speech Without Distortion," Electronics 47, 87 (1974).

Stark, H., Dimitriadis, B., "Minimum-Bias Spectral Estimation with a Coherent Optical Spectrum Analyzer," J. Opt. Soc. Am. 65, 425 (1975).

Thomas, C. E., "Optical spectrum analysis of large bandwidth signals," Applied Optics 5, 1782-1790 (1966).

Tierney, J., Gold, B., Sferrino, V., Dumanian, J., and Aho, E., "Channel vocoder with digital pitch extractor," J. Acoust. Soc. Am. 36, 1901-1905 (1964).

Vilbig, F., "Devices for speech analysis and compression," paper presented at the Fifth Annual National Electronics Conference in Chicago, 26-28 September 1949, published in Vol. V of the "Proceedings of the National Electronics Conference" (1950a).

_____ "An apparatus for speech compression and expansion and for replaying visible speech records," J. Acoust. Soc. Am. 22, 754-761 (1950b).

Whitman, R., Korpel, A., and Lotsoff, S., "Application of acoustic Bragg diffraction to optical processing techniques," presented at the Symposium on Modern Optics, Polytechnic Institute of Brooklyn, 22-24 March 1967, available from A. Korpel, Zenith Radio Corp., Chicago, Ill.

Yu, F. T. S., "Synthesis of an optical sound spectrograph," J. Acoust. Soc. Am. 51, 433-438 (1972).

E-21-640

GEORGIA INSTITUTE OF TECHNOLOGY
SCHOOL OF ELECTRICAL ENGINEERING
ATLANTA, GEORGIA 30332

TELEPHONE: (404) 894-2901

FINAL SUMMARY LETTER REPORT

NSF Grant GK-41222

Principal Investigator: Dr. William T. Rhodes

Starting Date: 1 February 1974

Completion Date: 31 July 1975

Grant Title: Two-Dimensional Optical Processing of One-Dimensional Signals

Brief Description of Research and Results: Results of this research project are reported in detail in the accompanying final technical report, TR No. GIT-EE-OIPL-75-1. The abstract of that report is reproduced here.

The research reported here centers on the investigation of a new class of coherent-optical processing operations for one-dimensional signals. In this class, the second degree of freedom provided by an optical system is utilized in performing operations largely new to signal processing. These operations have great potential in the development of specialized signal analysis devices--e.g. a constant relative bandwidth optical spectrum analyzer with log-frequency output display--and provide the basis for powerful frequency variant-frequency mapping signal waveform processing operations. Although the two-dimensional nature of coherent optical systems has been utilized before in the processing of on -dimensional signals, this utilization has been primarily to extend to signals of larger information content operations that can be performed by one-dimensional systems. By way of contrast, the operations reported here depend intrinsically on the two-dimensional nature of the optical system. Theoretical aspects of the research include an analytical modeling of the interaction of the different two-dimensional masks and holographic elements that serve as principle elements in the systems and a comparison of the optical techniques with other signal spectral analysis schemes. Several spectral analysis systems are investigated experimentally.

Potential Application to Engineering and Technology: Frequency variant-frequency warping spectrum analysis operations of the kind investigated in this project, especially the constant-Q log-frequency analysis, are particularly useful in the analysis of noise in rotating machinery and in the spectral analysis of doppler sonar and radar signals. Such analyses can be performed digitally, but only with computational difficulty (fast algorithms have not been

developed yet). Non-optical analog spectrum analyzers are comparatively limited with respect to the duration and bandwidth of the signal to be analyzed.

Personnel Involved in the Research: The research was conducted by the Principal Investigator, Dr. Rhodes, and by a Ph.D. candidate, Mr. James Florence. Basic concepts relating to the operation, design, and application of the optical systems were principally the contributions of the Principal Investigator, although it should be noted that discussions with Mr. Leonard Laub, who served as a consultant on the project, were very important to the clarification of certain ideas, particularly with respect to the general variable resolution-frequency mapping spectrum analyzer discussed in Section II of the technical report. Mr. Florence's contributions were primarily in the mathematical modeling of these systems and in the relating of their output to time-frequency signal energy distribution concepts discussed in the literature (see Section III of the technical report). His contributions in this latter area will be particularly important to followon phases of the research. Mr. Florence has also participated actively in the experimental aspects of the research.

Papers in Preparation: The final technical report was written in such a way that three journal publications will result with little modification--

> "Log-Frequency Optical Spectrum Analyzer Using a Holographic Mapping Element," to be submitted to Optics Communications.
>
> "Two-Dimensional Optical Processing of One-Dimensional Signals," to be submitted to Applied Optics.
>
> "Time-Frequency Spectral Analysis with Two-Dimensional Optical Systems," to be submitted to IEEE Transactions on Acoustics, Speech, and Signal Processing.

The first two papers will be submitted almost immediately. The third will require another month or so for preparation.

Inventions or Discoveries: During the course of this research, several new and potentially very useful techniques for coherent optical spectrum analysis were either conceived or first reduced to practice. The holographic mapping log-frequency spectrum analyzer, discussed in Appendix A of the TR, although conceived well before the grant period, was first demonstrated under NSF support. The more general frequency variant-frequency mapping spectrum analyzer described in Section II of the TR was both conceived and demonstrated with Foundation support. These ideas have some possible commercial value of their own and are expected to be quite important to later signal processing operations to be investigated. As such, they may deserve patent consideration.

Final Report on Grant GK-41222 submitted by

Dr. William T. Rhodes
Assistant Professor
School of Electrical Engineering
Georgia Institute of Technology
Atlanta, Georgia 30332
(404) 894-2929

30 July 1975

E-21-640

GEORGIA INSTITUTE OF TECHNOLOGY
SCHOOL OF ELECTRICAL ENGINEERING
ATLANTA, GEORGIA 30332

TELEPHONE: (404) 894-2901

July 30, 1975

Mr. Elias Schutzman, Program Director
Electrical and Optical Communications
Program
National Science Foundation
Washington, D.C. 20550

Subject: Final Report on Grant GK-41222

Dear Mr. Schutzman:

During the past several weeks I have worked to complete the final technical report on my NSF supported research project, Two-Dimensional Optical Processing of One-Dimensional Signals, grant GK-41222. Two bound, high-quality xerox copies of this report are enclosed; additional printed copies will be available in several weeks time.

I am somewhat embarrassed to submit it at the last minute this way. As I may have mentioned to you on an earlier occasion, however, I am coauthoring a textbook on lasers and their applications with two other Georgia Tech faculty. During the past four months we have been struggling to complete the manuscript in time for a 1976 publication date (Addison Wesley is publishing). We have found the task beyond our capabilities; and at the same time work on reports and journal publications has been laid aside. One reason for preparation of the lengthy technical report on a one-year grant has been to consolidate research results in form suitable for immediate publication. Our findings have been communicated verbally at several conferences now, including a meeting of the O.S.A. and last summer's Gordon Conference. The time is long overdue for a widely distributed written report on the work, however.

I am basically pleased with the results of our effort under this grant and sincerely hope we have the opportunity to continue with planned phases. I am encouraged by your recent word that reviews of my proposal for follow-on support are generally positive.

Also enclosed are the requisite two copies of the Summary Letter report, which augments the technical information contained in the more lengthy technical report. I call to your attention the portion concerning inventions and discoveries. You may want to discuss the subject with me over the phone.

I want to express my deep personal gratitude for the support I have received from the Foundation and to you for your efforts in securing this support. I have found research on this project most rewarding: the topic has been and continues to be very exciting, providing both me and my graduate

students excellent opportunity for meaningful and challenging work.

Sincerely,

William T. Rhodes
Assistant Professor

WTR:kak

Enclosures